



**HAL**  
open science

# **A biomechanical model of cardinal vowel production: muscle activations and the impact of gravity on tongue positioning**

Stéphanie Isabelle Buchaillard, Pascal Perrier, Yohan Payan

► **To cite this version:**

Stéphanie Isabelle Buchaillard, Pascal Perrier, Yohan Payan. A biomechanical model of cardinal vowel production: muscle activations and the impact of gravity on tongue positioning. *Journal of the Acoustical Society of America*, 2009, 126 (4), pp.2033-2051. 10.1121/1.3204306 . hal-00422426

**HAL Id: hal-00422426**

**<https://hal.science/hal-00422426>**

Submitted on 7 Oct 2009

**HAL** is a multi-disciplinary open access archive for the deposit and dissemination of scientific research documents, whether they are published or not. The documents may come from teaching and research institutions in France or abroad, or from public or private research centers.

L'archive ouverte pluridisciplinaire **HAL**, est destinée au dépôt et à la diffusion de documents scientifiques de niveau recherche, publiés ou non, émanant des établissements d'enseignement et de recherche français ou étrangers, des laboratoires publics ou privés.

**A biomechanical model of cardinal vowel production: muscle activations and the impact of gravity on tongue positioning**

Stéphanie Buchaillard<sup>a)</sup> and Pascal Perrier<sup>b)</sup>

*ICP/GIPSA-lab - UMR CNRS 5216 - Grenoble INP (France)*

Yohan Payan<sup>c)</sup>

*TIMC-IMAG - UMR CNRS 5525 - Université Joseph Fourier - Grenoble (France)*

(Dated: July 21, 2009)

## **Abstract**

A 3D biomechanical model of the tongue and the oral cavity, controlled by a functional model of muscle force generation ( $\lambda$ -model of the equilibrium point hypothesis) and coupled with an acoustic model, was exploited to study the activation of the tongue and mouth floor muscles during the production of French cardinal vowels. The selection of the motor commands to control the tongue and the mouth floor muscles was based on literature data, such as electromyographic (EMG), electropalatographic (EPG) and cineradiographic data. The tongue shapes were also compared to data obtained from the speaker used to build the model. 3D modeling offered the opportunity to investigate the role of the transversalis, in particular its involvement in the production of high front vowels. It was found, with this model, to be indirect via reflex mechanisms due to the activation of surrounding muscles, not voluntary. For vowel /i/, local motor command variations for the main tongue muscles revealed a non-negligible modification of the alveolar groove in contradiction to the saturation effect hypothesis, due to the role of the anterior genioglossus. Finally, the impact of subject position (supine or upright) on the production of French cardinal vowels was explored and found to be negligible.

PACS numbers: 43.70.Aj, 43.70.Bk

## I. INTRODUCTION

Speech movements and acoustic speech signals are the results of the combined influences of communicative linguistic goals, perceptual constraints and physical properties of the speech production apparatus. To understand how these different factors combine and interact with each other, it requires an efficient approach that develops realistic physical models of the speech production and/or speech perception systems. The predictions of these models can then be compared with experimental data, and used to infer information about parameters or control signals that are not directly measurable or the measurement of which is difficult and not completely reliable. Such a methodological approach underlies the present work, in which a biomechanical model of the vocal tract has been used to study muscle control in vowel production, its impact on token-to-token variability and its consequences for tongue shape sensitivity to changes in head (supine versus upright) orientation. The findings are interpreted in the light of our own experimental data and data published in the literature.

Biomechanical models of the tongue and vocal tract have been in use since the 1960's, and their complexity has increased with the acquisition of new knowledge about anatomical, neurophysiological and physical characteristics of the tongue, as well as with the vast growth in the computational capacities of computers. All these models have significantly contributed to the increase in knowledge about tongue behavior and tongue control during speech production, and more specifically about the relations between muscle recruitments and tongue shape or acoustic signal (see in particular Perkell, 1996, using his model presented in Perkell (1974); Kakita *et al.*, 1985; Hashimoto and Suga, 1986; Wilhelms-Tricarico, 1995; Payan and Perrier, 1997; Sanguineti *et al.*, 1998; Dang and Honda, 2004). With a more sophisticated 3D vocal tract model, based on non-linear continuum mechanics modeling, and taking in consideration a number of recent experimental findings, this study aims at deepening and extending these former works for vowel

---

a) [Stephanie.Buchillard@gipsa-lab.inpg.fr](mailto:Stephanie.Buchillard@gipsa-lab.inpg.fr)

b) [Pascal.Perrier@gipsa-lab.inpg.fr](mailto:Pascal.Perrier@gipsa-lab.inpg.fr)

c) [Yohan.Payan@imag.fr](mailto:Yohan.Payan@imag.fr)

production.

The model consists of a 3D biomechanical model of the tongue and the oral cavity, controlled by a functional model of muscle force generation ( $\lambda$ -model of the equilibrium point hypothesis) and coupled with an acoustic model. It is a significantly improved version of the model originally developed in GIPSA-lab by Gérard and colleagues (Gérard *et al.*, 2003; Gérard *et al.*, 2006). The oral cavity model was developed so as to give as realistic a representation as possible of the anatomy and of the mechanical properties of the oral cavity. The original modeling was based on the data of the Visible Human Project, and further adapted to the anatomy of a specific subject. For this subject, different kinds of data (X-ray, CT images, acoustic data) were available. The parameters used in this model were either extracted from the literature, derived from experimental data or adapted from the literature. This modeling study is inseparable from a thorough experimental approach. In addition to a careful and accurate account of anatomical, mechanical and motor control facts, the model implements a number of hypotheses about the hidden parts of the speech production system. Simulation results, their interpretation and the corresponding conclusions aim at opening new paths for further experimental research that could validate or contest these conclusions.

The main characteristics of the model (geometry, mechanical properties and model of control) are presented in Section II. The model includes improvements in the anatomical and morphological description and in the strain/stress function, as well as a control model of muscle activation (Section II). The model is first used (Section III) in order to characterize the muscle activation patterns associated with the production of the French cardinal vowels. Starting from these patterns, the relation between internal muscle strain and muscle activations is systematically studied. In the following section (Section IV), the sensitivity of the postural control of the tongue (and hence of the formant frequencies) to changes in motor commands is precisely studied for /i/, which is often described in the literature as a very stable vowel due to specific combinations of muscle activations. Finally, the impact on tongue positioning of changes in gravity orientation is assessed (Section V). Perspectives and further developments are discussed in the conclusion.

## II. MODELING THE ORAL CAVITY

Modeling the oral cavity by a finite element approach requires meshing the structure of interest, specifying its mechanical properties, and defining a motor control scheme. Then, the simulation of movements in response to motor commands requires solving the body motion equations. These different aspects will be described in this section.

The primary goal of our work is the development of a model which allows a better understanding of how motor control and physical aspects combine and interact to determine the characteristics of speech production signals. Hence, a high degree of realism is essential in the design of the model, not only concerning the geometrical properties, but also the mechanical and control aspects.

The model described below is an improved version of the model developed by Gérard and colleagues (Gérard *et al.*, 2003; Gérard *et al.*, 2006). The original model was based on the Visible Human Project® data for a female subject and the work of Wilhelms-Tricarico (2000). It was then adapted to a specific male subject, PB henceforth. Major differences between the current version and those of Gérard and colleagues lie in (1) the motor control scheme (muscle forces are now computed via the  $\lambda$ -model of the equilibrium point hypothesis), (2) the constitutive law for the tongue tissues (the law inferred by Gérard *et al.* (2005) from indentation measurements of fresh cadaver tissues was modified to match the properties of living tissues; in addition, the law now depends on the level of muscle activation), (3) the modeling of the hyoid bone (a new scheme was also developed to deal with hyoid bone mobility and to model the infrahyoid and digastric muscles). Modifications were also made to the tongue mesh, the muscle fibers, the bony insertions and the areas of contact between the tongue and the surrounding surfaces, namely the mandible, the hard palate and the soft palate. The 3D vocal tract model was also coupled with an acoustic model.

## A. Geometrical and anatomical structures

A precise description of the tongue anatomy will not be given here. A thorough description, which lies at the root of this work, can be found in Takemoto (2001). The tongue model represents the 3D structure of the tongue of a male subject (PB), for whom several sets of data have been collected in the laboratory in the last 15 years. This model is made of a mesh composed of hexahedral elements. The anatomical location of the major tongue muscles is specified via subsets of elements in the mesh. Fig. 1 shows the implementation of the 11 groups of muscles represented in the model and known to contribute to speech production. Nine of them exert force on the tongue body itself, while the other two, depicted in the last two panels (Fig. 1(j) and 1(k)), are considered to be the major mouth floor muscles. Of course, due to the elastic properties of tongue tissues, each muscle is likely to induce strain in all the parts of the tongue and mouth floor. On rare occasion the muscle shape is somewhat unnatural because the tongue muscles were defined as a subset of elements of the global mesh. This is for example the case with the IL. However, when activated, the force generated by the IL appeared correct in amplitude and direction. The insertion of the different parts of the genioglossus on the mandible can also appear odd: in human beings, GGp emanates from the lower surface of the short tendon that reduces crowding of the fibers at the mandibular symphysis by allowing GGp to arise from below and the radial fibers to arise from above. In the model, the tendon is not represented and the origins of GGp, GGm and GGa are all on the mandibular symphysis. This results in a somewhat too large region of insertion on the mandible. Only a refined mesh structure would allow a better muscle definition in this area.

It is generally accepted that a muscle can possibly be divided in a number of functionally independent parts. For tongue muscles this possibility exists, but little work has been done in the past concerning this issue. Some proposals were the results of *ad hoc* choices made in order to explain measured 2D or 3D tongue shapes (e.g. the most recent proposal for the styloglossus in Fang *et al.*, 2008). Some more physiologically based studies used EMG signals, generally assuming that these signals reflect the underlying motor control. Among these studies, the one carried out by Miyawaki *et al.* (1975) showed evidence for different activities in different parts of the

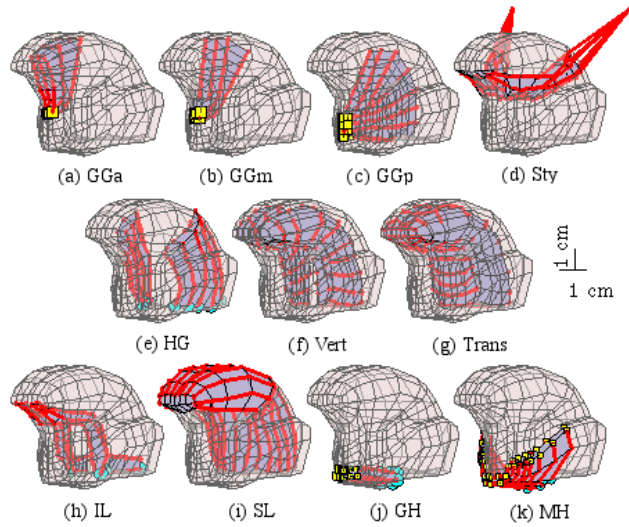


FIG. 1. (color online) Mesh representation (gray elements) of lingual and mouth floor muscles as subsets of tongue elements (global mesh) (anterior oblique view). (a-c) anterior, medium and posterior part of the genioglossus, (d) styloglossus, (e) hyoglossus, (f) verticalis, (g) transversalis, (h) inferior longitudinalis, (i) superior longitudinalis, (j) geniohyoid, (k) mylohyoid. The muscle fibers are represented in red. The yellow squares and the blue dots represent the muscle insertions on the mandible and the hyoid bone, respectively.

genioglossus. However, EMG activity is the result of a combination of efferent and afferent influences and it cannot be seen as a direct image of the underlying control. In addition, as emphasized by Miyawaki *et al.* (1975), if subdivisions exist in a muscle, we do not know in what manner they are voluntarily controlled (p. 101). We believe that the only reliable way to address this issue would be to look at the motor unit distribution within tongue muscles. To our knowledge, we lack information on the localization of motor unit territories in human tongue muscles. One way to know more about it could be to study the architecture of the muscles, with the underlying hypothesis that structurally separated muscle parts could be innervated by independent motor units. Slaughter *et al.* (2005) have carried out such a study for the human SL, and they found that this muscle consists of a number of in-series muscle bundles that are distributed along the front-back direction. However, they could not provide clear evidence for the fact that these muscle bundles are innervated by independent motor units. In the absence of convincing physiological evidence,



and in order to limit the complexity of the model, only the genioglossus, for which a consensus seems to exist, was subdivided: three independent parts called the GGa (anterior genioglossus), the GGm (medium genioglossus), and the GGp (posterior genioglossus) were thus defined.

To mesh the hard and soft structures forming the oral cavity, data of different kinds such as computed tomography (CT) scans, magnetic resonance imaging (MRI) data and X-ray data, all collected for PB, were exploited. In addition to the tongue and mouth floor meshes, the model (Fig. 2) includes a surface representation of the mandible, the soft palate, the hard palate and the pharyngeal and laryngeal walls as well as a volumetric mesh (tetrahedral elements) of the hyoid bone. A set of 6 pairs of springs (right and left sides), emerging from the hyoid bone, are used to represent the elastic links between this mobile bone and fixed bony structures associated with the anterior and posterior belly of the digastric, infrahyoid muscles (sternohyoid, omohyoid and thyrohyoid muscles) as well as the hyo-epiglottic ligaments.

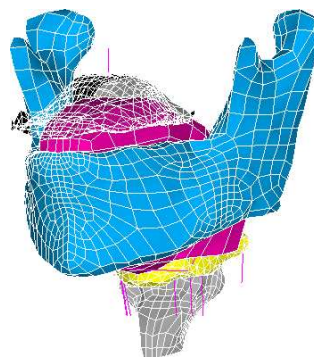


FIG. 2. (color online) Oblique anterior view of the 3D tongue mesh in the whole oral cavity for a rest position (tongue mesh in magenta, mandible in cyan, hyoid bone in yellow, translucent soft palate, pharyngeal and laryngeal walls in gray, infra- and supra-hyoid muscles represented as magenta lines).

The relative positions of the different articulators were carefully adjusted so as to represent well PB's morphology in a seated position and at rest, just as they are described by lateral X-ray views of PB's oral cavity. The final tongue shape in the midsagittal plane at rest was also adapted so as to match the corresponding X-ray view. This induced some geometrical changes to the original shape proposed in Gérard *et al.* (2006), because the MRI data used for the original design

of that model corresponded to the subject in the supine position; gravity was then shown in that case to influence tongue shape.

## **B. Mechanical properties**

The lingual tissues were modeled with a non-linear hyper-elastic constitutive law, more precisely a 2<sup>nd</sup> order Yeoh constitutive law (Gérard *et al.*, 2005, 2006). Two different constitutive equations were introduced: one describes the passive behavior of tongue tissues and the other one models the strain/stress relation for active muscle tissues as an increasing function of muscle activation. For a particular mesh element, the passive or the active constitutive law is used according to whether this element belongs to a passive or to an active region (i.e a region made of activated muscle(s)). The passive constitutive law was directly derived from the non-linear law proposed by Gérard *et al.* (2005), which was derived from measurements on a fresh cadaver. However, since the stiffness of tissues measured shortly after death is known to be lower than that measured in *in vivo* tissues, the constitutive law originally proposed by Gérard *et al.* (2005) was modified.

To our knowledge, one of the most relevant *in vivo* measurements of human muscle stiffness is the one carried out by Duck (1990), who proposed a value of 6.2 kPa for the Young modulus for a human muscle at rest, and a maximum value of 110 kPa for the same muscle once contracted. The Young modulus measured by Gérard *et al.* (2005) on a cadaver tongue at low strain is 1.15 kPa, which is significantly smaller than Duck's *in vivo* measures. This difference is not surprising, since in living subjects a basic muscle tonus exists, even at rest. Hence, it was decided to multiply both 2<sup>nd</sup> order Yeoh law coefficients originally proposed by Gérard *et al.* (2005) by a factor of 5.4, in order to account properly for the Young modulus at rest measured by Duck (1990). Multiplying both coefficients by the same factor allows preserving the overall non-linear shape of the Yeoh constitutive law (Fig. 3). This new law specifies the properties of passive tongue tissues. In order to account for the stiffening associated with muscle activation as measured by Duck (1990), it was decided for the elements belonging to an activated muscle to multiply the coefficients of the Yeoh constitutive law for passive tissues by a factor that is a function of muscle activation. Thus,

an activation-related constitutive law was defined for the active muscles. The multiplying factors were chosen by taking into account the fact that the contributions of the different muscles to the Young modulus of an element combine in an additive manner. The basic idea is that an activation of a muscle leads to an increase in its Young modulus. Given  $c_{10,r}$  and  $c_{20,r}$  the Yeoh parameters for tongue tissues at rest, the parameters  $c_{i0}(e, t)$  ( $i \in \{1, 2\}$ ) at time  $t$  for an element  $e$  belonging to the tongue or mouth floor, are given by:

$$c_{i0}(e, t) = c_{i0,r} \left( 1 + \sum_{\text{muscles } m} p_1(m) \left[ \sum_{\text{fibers } f \in m} A(f, t) \times p_2(f, e) \right] \right) \quad (1)$$

with  $p_1$  a positive muscle-dependant factor,  $A(f, t)$  the activation level for the macrofiber  $f$  at time  $t$  (see the Eq. 2 below) and  $p_2(f, e)$  a factor equal to 1 if  $e$  belongs to  $m$  and if the fiber  $f$  runs along the edges of  $e$ , 0 otherwise.

The multiplying factor  $p_1$  were chosen in order to maintain the stiffness value below 110 kPa, when maximal muscle activation is reached.

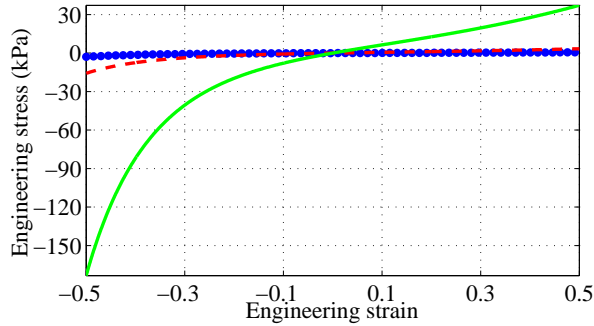


FIG. 3. (color online) Stress/strain hyperelastic constitutive law (Yeoh 2<sup>nd</sup> order material) for lingual tissues. The dotted curve represents the original law obtained from fresh cadaver tissues ( $c_{10} = 192$  Pa and  $c_{20} = 90$  Pa), the dashed curve the law used in the current model for passive tissues ( $c_{10} = 1037$  Pa and  $c_{20} = 486$  Pa) and the solid line the law used for the maximal activation ( $c_{10} = 10.37$  kPa and  $c_{20} = 4.86$  kPa).

Since tongue tissues are considered to be quasi-incompressible, a Poisson coefficient equal to 0.499 was used. Furthermore, tongue tissues density was set to  $1040 \text{ kg.m}^{-3}$ , close to water density.

Currently, only the tongue and the hyoid bone (with the springs connecting it to fixed bony structure) are modeled as movable structures and need to be mechanically characterized. The hyoid bone was considered as a rigid body and its density ( $2000 \text{ kg.m}^{-3}$ ) was estimated based on values published in the literature (Dang and Honda, 2004). The same stiffness coefficient ( $220 \text{ N.m}^{-1}$ ) was chosen for all the springs connecting the hyoid bone to solid structures; this value enabled us to reproduce displacements of the hyoid bone that were consistent with data published in Boë *et al.* (2006).

### **C. Motor control: Implementation of postural control with short latency feedback**

The motor control scheme implemented is based on the  $\lambda$  version of the equilibrium point hypothesis (EPH) (Feldman, 1986). This theory is known to be controversial in the motor control domain. The main criticisms are about the fact that this theory claims that the time variation of motor control variables does not result from any inverse kinematics or inverse dynamics processes (see for example Gomi and Kawato (1996) or Hinder and Milner (2003)). However, the defenders of the EPH theory have systematically provided refutations of these criticisms that support the value of the model in research (e.g. in Gribble and Ostry (1999) or Feldman and Latash (2005)). Our own work has also shown that speech motor control based on the equilibrium point hypothesis gives a good account of complex kinematic patterns with a 2D biomechanical model of the vocal tract (Payan and Perrier, 1997; Perrier *et al.*, 2003). From our point of view, this motor control theory seems particularly interesting for speech production because it provides the framework for a discrete characterization of continuous physical signals at a motor control level thanks to the link that can be made between successive equilibrium points and targets; it thus allows a connection to be made between the discrete phonological units and the physical targets that underlie continuous articulatory and acoustic signals (Perrier *et al.*, 1996). In addition, the equilibrium point hypothesis integrates short latency feedback to contribute to the accuracy of speech gesture, which is for us a crucial feature for speech production control (Perrier, 2006). Hence, the approach used in our previous modeling work with the 2D biomechanical model of the vocal tract was extended to the

3D model.

### ***1. Adjustment of feedback delay***

The implementation chosen for the EPH follows the approach proposed by Laboissière *et al.* (1996) and further developed by Payan and Perrier (1997). In the model, bundles of fibers are represented by way of *macrofibers* (specified as ordered lists of mesh nodes along the edges of elements) that represent the main directions of muscle fibers in the different parts of the tongue. In the current version of the model, a unique activation threshold was defined for each muscle (three for the genioglossus, which was divided into three parts that are assumed to be separately controlled: the anterior, posterior and medium parts). Every muscle was assumed to be controlled independently. Obviously, synergies and antagonisms exist in tongue muscles. However, there is no evidence in the literature supporting the hypothesis that these muscle coordinations are implemented in humans from birth. It is much more likely that coordinated muscle activations are the result of learning and that they could be task specific. Our modeling approach is in line with this statement. The design of our biomechanical model gives the largest possible number of degrees of freedom to the system to be controlled, and does not impose a priori hypotheses that could bias our study. It allows future work on the emergence of muscle coordinations through task specific learning. For each muscle, the motor command  $\lambda_{\text{muscle}}$  was determined for the longest macrofibers  $l_{\text{max}}$ ; the  $\lambda$  value for each macrofiber of the same muscle was then determined by simply multiplying the  $\lambda_{\text{muscle}}$  value by the ratio of the macrofiber length at rest over  $l_{\text{max}}$ .

For a given macrofiber, the muscle activation  $A$  takes into account the difference between the macrofiber length and the motor command  $\lambda$ , as well as the lengthening/shortening rate.

A stretch reflex delay  $d$ , which corresponds to the propagation delay for the electrical signals to travel along the reflex arc plus the synaptic time and the integration time of these signals at the interneurons, is taken into account for fiber length and velocity intervening in the computation of  $A$ . In their model of the mandible, Laboissière *et al.* (1996) proposed a delay of 10 ms, and in their tongue/jaw model Sanguineti *et al.* (1998) suggested a delay of 15 ms. In the present model,  $d$

was set to 17 ms, based on the data of Ito *et al.* (2004). Simulations conducted for  $d$  ranging from 5 ms to 20 ms showed that this value had a limited impact on tongue motion; the trajectory, peak velocity, acceleration or force levels were altered, but in a limited range so that the choice of this value did not seem to be critical within this range of variation. The sensitivity of the activation to the lengthening/shortening rate  $\dot{l}$  is modulated by a damping coefficient  $\mu$ , considered for the sake of simplicity as constant and identical for all the muscles.  $\mu$  was chosen to be equal to 0.01 s to ensure the stability of the system, following numerous simulations.

$$A(t) = [l(t-d) - \lambda(t) + \mu\dot{l}(t-d)]^+ \quad (2)$$

Muscle activation is associated with the firing of the motoneurons (henceforth MNs). Hence  $A$  is either positive or zero (if  $A$  is mathematically negative, it is set to zero). A zero value corresponds to the MNs fire threshold; beyond this threshold, the MN depolarization becomes possible: the higher the activation  $A$ , the higher the firing frequency of MNs. As long as the activation  $A$  is zero, no force is generated. Force varies as an exponential function of the activation (see below).

## 2. Feedback gain: A key value for postural control stability

Active muscle force  $\tilde{M}$  is given as a function of the activation  $A(t)$  by the following equation:

$$\tilde{M}(t) = \max \left[ \rho \left( \exp^{cA(t)} - 1 \right), \rho \right] \quad (3)$$

with  $\rho$  a factor related to the muscle capacity of force generation and  $c$  a form parameter symbolizing the MN firing gradient.

The determination of the parameter  $\rho$ , which modulates the force generation capacity, is based on the assumption that, for a fusiform muscle,  $\rho$  is linked in a first approximation to the cross-sectional area of the muscle. The values are based on the work of Payan and Perrier (1997) for the tongue muscles, except for the transversalis, which was non-existent in a 2D tongue model, and with some adaptations for the verticalis, the implementation of which was slightly different. For the mouth floor muscles  $\rho$  values were estimated from the data from van Eijden *et al.* (1997),

and were measured on the model for the transversalis. This muscle force capacity (Table I) was distributed among the different macrofibers proportionally to the volume of the surrounding elements. Given a fiber  $f$  belonging to a muscle  $m$ , its capacity of force generation  $\rho_{\text{fib}}$  is such that:

$$\rho_{\text{fib}}(f) = \rho(m) \frac{\sum_e V(e) \times p(e, f)}{S} \quad (4)$$

with  $e$  an element belonging to  $m$ ,  $V(e)$  the volume of  $e$ ,  $p(e, f)$  a parameter equal to 1 if  $f$  is located inside the muscle, 0.5 on a muscle face (exterior surface of a muscle excluding muscle corners) and 0.25 on a muscle edge (exterior surface of a mesh, corners only).  $S$  is a normalization term, such that the  $\rho_{\text{fib}}$  values for the different fibers of  $m$  sum up to  $\rho(m)$ .

Parameter  $c$  is an important factor for stability issues since it determines how feedback information included in the activation influences the level of force. Original values for  $c$  found in the literature ( $c = 112 \text{ m}^{-1}$ , Laboissière *et al.*, 1996) brought about dramatic changes in the muscular activation level for a small variation in the muscle length. This generated mechanical instabilities. Therefore, parameter  $c$  was decreased. After several trials,  $c$  was fixed to  $40 \text{ m}^{-1}$ . This value is not the only one that ensured a stable mechanical behavior of the model. A large range of values was possible. The value  $40 \text{ m}^{-1}$  was chosen because it provides a fair compromise between the level of reflex activation and stability (Buchillard *et al.*, 2006).

The influence of muscle lengthening/shortening velocity on the force developed is also included. The model accounts for the sliding filaments theory (Huxley, 1957) by calculating the total muscle force  $F$  with the following equation (Laboissière *et al.*, 1996):

$$F(t) = \tilde{M}(t) \left( f_1 + f_2 \arctan \left( f_3 + f_4 \frac{\dot{l}(t)}{r} \right) + f_5 \frac{\dot{l}(t)}{r} \right) \quad (5)$$

where  $\dot{l}$  is the lengthening/shortening velocity and  $r$  the muscle length at rest. The parameters used are based on the work of Payan and Perrier (1997) for rapid muscles, but are slightly different:  $f_1 = 0.7109$ ,  $f_2 = 0.712$ ,  $f_3 = 0.43$ ,  $f_4 = 0.4444 \text{ s}$ ,  $f_5 = 0.0329 \text{ s}$ .

#### D. Lagrangian equation of motion and boundary conditions

The Lagrangian equation of motion that governs the dynamic response of the finite element system is given by:

$$\mathbf{M}\ddot{\vec{q}} + \mathbf{C}\dot{\vec{q}} + \mathbf{K}\vec{q} = \vec{F} \quad (6)$$

with  $\vec{q}$  the nodal displacements vector,  $\dot{\vec{q}}$  and  $\ddot{\vec{q}}$  its first and second derivatives,  $\mathbf{M}$  the mass matrix,  $\mathbf{C}$  the damping matrix,  $\mathbf{K}$  the stiffness matrix and  $\vec{F}$  the load vector (the reader can refer to Bathe (1995) for a detailed description of the Finite Element Method).

A Rayleigh damping model was chosen for the definition of the damping matrix :  $\mathbf{C} = \alpha\mathbf{M} + \beta\mathbf{K}$ .  $\alpha$  and  $\beta$  were set to  $40 \text{ s}^{-1}$  and  $0.03 \text{ s}$ , respectively, in order to have a damping close to the critical one in the range of modal frequency from 3 to 10 Hz (Fig. 4).

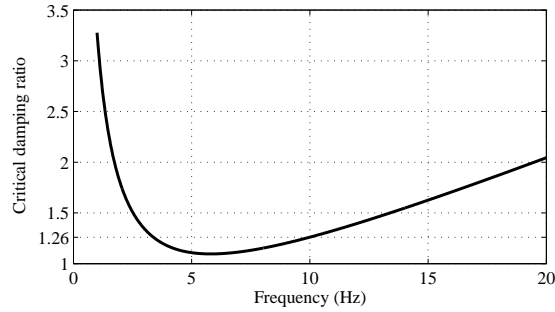


FIG. 4. Ratio damping over critical damping vs. frequency for  $\alpha = 40 \text{ s}^{-1}$  and  $\beta = 0.03 \text{ s}$  (Rayleigh damping model). For a modal frequency from 3 to 10 Hz, the damping ratio is below 1.26, i.e. close to the critical damping (ratio equal to 1).

The load vector  $F$  includes the muscle forces computed for every macrofiber (Eq. 5), the gravity and contact forces between tongue and vocal tract walls.

Two kinds of boundary conditions were introduced through the definition of no-displacement constraints to model muscular insertions and the management of contacts. Muscle insertions on the bony structures (inner anterior and lateral surface of the mandible and hyoid bone) were implemented and they match as well as possible the information about PB's anatomy that was extracted from X-ray scans. During speech production, the tongue comes into contact with the hard and soft



tissues that compose the vocal tract walls. Consequently, the contacts were modeled between the tongue and the set hard palate/upper dental arch, the soft palate and the set inner surface of the mandible/lower dental arch. The modeling of contacts is non-linear. A face-to-face detection was used to avoid the interpenetration of the surfaces in contact, which are potentially in contact with the tongue. A relatively low Coulomb friction was used, since friction is assumed to be limited due to the saliva. The contacts are managed through an augmented Lagrangian method, which corresponds to an iterative series of penalty methods.

The partial differential equation (6) was solved by the Ansys<sup>TM</sup> finite element software package, based on a combination of Newton-Raphson and Newmark methods.

## **E. Acoustic modeling**

A model of sound synthesis, including the determination of the 3D area function of the vocal tract, was coupled with the mechanical model.

The computation of the area function from the mesh node coordinates was achieved by using the Matlab<sup>®</sup> software. Before computing the area function, the surface of the tongue was interpolated using 35 periodic cubic splines in order to get a more accurate detection of the constriction locations in the vocal tract. This processing and its use for the computation of the area function make the implicit assumption that the spatial sampling of the tongue surface provided by the finite element mesh is sufficient to allow a correct interpolation of the tongue surface from the positions of the nodes. A set of planes, which will be referred to as cutting planes below, was computed for the vocal tract in its rest position. These cutting planes, orthogonal to the sagittal plane, are approximately perpendicular to the vocal tract midline at rest. For a given vocal tract configuration, the intersections between the cutting planes and the surface of the tongue (approximated by a set of periodic cubic splines), of the mandible, of the hyoid bone, of the hard and soft palates, and of the pharyngeal and laryngeal walls were computed. On every cutting plane, a closed contour based on these intersections and representing the shape of the vocal tract was computed and approximated by periodic cubic splines. The inner surface of each of the thus determined closed contours was

calculated. The lips, which are not part of the biomechanical model, were represented by a single cylinder, whose length and section represented lip protrusion and aperture, respectively. To determine the distance between two consecutive cutting planes, and thus to compute the length of the path from the glottis to the lips, it was decided to compute the distance between the centers of gravity of two successive surfaces. This distance approximates the average distance traveled by the acoustic wave between two consecutive cutting planes. An acoustic model (analog harmonic of the vocal tract) was used to generate the spectrum of the signal produced from the area function<sup>1</sup>.

### III. MUSCLE ACTIVATIONS DURING FRENCH ORAL VOWEL PRODUCTION

#### A. Muscle activations

To study the postural control of speech sounds, the best approach would consist in roaming the motor command space of the biomechanical model in a systematic and comprehensive way, using for example a Monte Carlo method, in order to characterize the links between motor commands, tongue shapes and acoustics, following the approach of Perrier *et al.* (2005) for their 2D model. However, such an approach is currently impossible with this 3D model, because of the running time (around 40 minutes for a 100 ms simulation, with Ansys<sup>TM</sup>11.0 and Windows XP SP2 running on a Pentium IV CPU at 3 GHz and 1 Go of RAM). Consequently, it was necessary to work with a more limited number of simulations to study muscle activations in vowel production and the sensitivity of the vowel configurations to changes in motor commands. The results presented in this section were obtained on the basis of 300 simulations, all carried out with a fixed mandible. These simulations resulted from a specific choice of motor commands guided primarily by studies with our model of the individual impact of each muscle on tongue shape (see below). Our objectives were to generate a very good match of the tongue shapes classically observed in the midsagittal plane for French oral vowels by means of cineradiographic data (Bothorel *et al.*, 1986). EMG studies by Miyawaki *et al.* (1975) and Baer *et al.* (1988) were also used as sources of complementary information on the main tongue and mouth floor muscles activated during vowel production. Acoustic signals were synthesized from the final vocal tract shape, and the formants

were calculated.

The selection of the optimal vowels has involved a mostly qualitative evaluation of the similarity between the computed tongue shapes and the 3D tongue shapes measured for the speaker PB (CT data). A quantitative comparison of the simulated tongue shapes with the measured 3D shapes was not possible and would not have been very informative, mainly for two reasons:

1. In our vocal tract model the jaw is fixed. It is known that a variety of jaw positions are possible for the same sound without endangering the quality of its perception, and, in particular, producing speech with a fixed jaw does not prevent the speakers from producing satisfactory vowels with fair formants, as shown by bite block experiments (Mooshammer *et al.*, 2001); however this articulatory perturbation has an impact on the tongue shape considered in its entirety.
2. The model is a symmetrical one while human subjects are never symmetrical. Hence a detailed comparison of the constriction shape was not possible. This is why our simulations were essentially assessed in terms of global tongue elevation, proximity to the palate, and front/back position of the constriction in the vocal tract. However, a quantitative evaluation of the simulated and measured formant patterns was carried out.

Only the simulations obtained for the extreme vowels /i, a, u/ will be presented in this paper. The results correspond to the shape and position of the tongue at the end of the simulated movement. For single muscle activations, movement lasted 400 ms while it lasted only 200 ms for the vowels (for the three vowels, steady state equilibrium positions were reached). In all cases, the movement started from rest position.

### ***1. Impact of individual muscles on tongue shape***

Figs. 5 and 6 show the individual impact of the tongue and mouth floor muscles on the tongue shape in the midsagittal plane and in the 3D space from a front view perspective. Target motor commands were defined such that a single muscle was activated during each simulation. For the

only activated muscle, the command (i.e., the threshold muscle length above which active muscle force is generated) was set either to 75% or 85% of the muscle length at rest (the smaller the percentage, the larger the activation; hence, a larger percentage was chosen for larger muscles to avoid too strong deformations). For the other muscles, the motor commands were set to a large enough value so as to prevent these muscles from generating forces; for example, a command twice as large as the muscle length at rest ensures that this muscle will remain inactive throughout a simulation. These simulations show that the role of the individual muscles in our model matches well with classic knowledge inferred from experimental data and clarify their impact on the tongue shape. The anterior genioglossus moves the tongue downward in its front part, essentially in the region close to the midsagittal plane (tongue grooving in the palatal region  $\approx 6$  mm). This downward movement is associated with a slight backward movement in the pharyngeal region (Fig. 5(a),  $\approx 1.6$  mm). Note that the backward movement is much smaller than the one predicted by 2D (Payan and Perrier, 1997) or 2.5D (Dang and Honda, 2004) models. This can be explained by the fact that in these models the volume conservation is in fact implemented as a surface conservation property in the midsagittal plane. In our model, volume conservation causes the changes that are generated in one part of the tongue to be compensated not only in the other parts of the midsagittal plane, but also in the whole tongue volume. Indeed, a slight enlargement of the tongue is observed in the transverse direction (up to 2.2 mm). It can also be noticed that the limited backward motion is consistent with data showing that a larger expansion may occur in the transverse plane, local to the compression, while a small expansion occur in the same plane (Stone *et al.*, 2004). The medium part of the genioglossus lowers the tongue in its dorsal region ( $\approx 5$  mm) and moves the apical part forward ( $\approx 3$  mm) and upward, while an enlargement of the tongue is observed in the transverse direction (up to 1.4 mm). The posterior genioglossus (GGp) enables the tongue to be pushed forward ( $\approx 5.3$  mm); this forward movement is associated with an elevation of the tongue ( $\approx 2.4$  mm) due to the apex sliding on the anterior part of the mandible (Fig. 5(c)). However, the elevation of the tongue is less strong than what was predicted by the 2D and the 2.5D models. As for the GGa, it leads to the enlargement of the tongue in the transverse direction ( $\approx 1.3$  mm in the apical area and 1.6 mm in the pharyngeal area, Fig. 6(c)). The styloglossus (Sty) causes

a downward ( $\approx 9.6$  mm) and backward ( $\approx 7$  mm) displacement of the tongue tip, producing an elevation of the dorsal part of the tongue and a lowering of the apical region (Figs. 5(d) and 6(d)). No change is observed in the transverse direction. Changes in the midsagittal plane are similar to the predictions of 2D or 2.5D models. The hyoglossus generates a backward movement in the pharyngeal part ( $\approx 5$  mm), an apex elevation (upward displacement of  $\approx 4.7$  mm) and a lowering of the tongue in its dorsal part (Fig. 5(e)). An enlargement is observed in the transverse direction in the pharyngeal part (Fig. 6(e),  $\approx 5$  mm). The verticalis provokes only a very small lowering in the palatal region (below  $\approx 0.5$  mm) associated with a very slight backward movement in the pharyngeal part (below  $\approx 0.5$  mm) (Fig. 5(f)). Its contraction also widens the tongue ( $\approx 1.4$  mm in the apical area). Its impact will then be essentially indirect: by stiffening its elements in the palatal part of the tongue, it will modify the action of other muscles. The transverse muscle induces essentially a reduction in the tongue width in the transverse direction (up to 2.1 mm in the superior part of the tongue, Fig. 6(g)). Due to the volume conservation property this change spreads over the whole tongue in the midsagittal plane, generating at the same time a small forward movement of the apex and a small backward movement in the pharyngeal part. The inferior longitudinalis lowers the tongue tip ( $\approx 5$  mm) and moves it backwards ( $\approx 6$  mm). A small backward movement of the tongue is also observed in the pharyngeal region ( $\approx 1.3$  mm) (Fig. 5(h)). In the transverse direction, a slight enlargement is observed in the dorsal region ( $\approx 1$  mm). The activation of the superior longitudinalis mainly induces an elevation ( $\approx 12$  mm) and a backward movement ( $\approx 11$  mm) of the tongue tip with a slight backward movement in the pharyngeal part ( $\approx 1.7$  mm) (Fig. 5(i)). The geniohyoid essentially moves the hyoid bone forward and downward, which induces a slight lowering in the dorsal region ( $\approx 0.7$  mm) (Fig. 5(j)). Finally, the mylohyoid elevates the mouth floor in its midsagittal part (up to 4 mm) and moves the dorsal part of the tongue slightly upward (Fig. 5(k)). The analysis of the influences of individual tongue muscles revealed possible synergies and antagonisms between muscles: GGp, Sty and GH can act in synergy to produce an elevation of the tongue in the palatal region; in this part of the tongue they act antagonistically with the GGa and the GGm. The Sty and GGm are antagonists for the control of the vertical position of the dorsal part of the tongue. The GGp, SL and GGm contribute to the tongue tip elevation and

their action can be counteracted by that of the IL, the Sty and the GGa. As for the control of the width of the tongue in the transverse direction, Trans tends to reduce it in the whole tongue body; GGa and GGm are the main muscles enlarging it in the palatal part, while HG contributes to its enlargement in the pharyngeal part.

## *2. Simulations of French vowels*

In order to generate the 300 simulations used to determine the muscle activation patterns for the French vowels, the timing of the motor commands was as follows: at time  $t = 0$ , the central commands were equal to the muscle length at rest; then they varied linearly for a transition time of 30 ms up to the target values. Coarse sets of motor commands were first determined for each vowel, guided by prior knowledge of the tongue shapes and by literature data. The values of the commands for the main muscles involved in the production of the vowels were then made to vary within a more or less wide range around their primary value. The range was determined according to the tongue shape sensitivity to their modification.

Within the set of 300 simulations, the best motor commands for French extreme vowels (Table III) were selected on the basis of the obtained tongue shapes and the formant patterns. Optimal vowels were chosen in order to get the best match between the tongue shape in the midsagittal plane with PB's MRI data, and between the formants computed with the formants measured from PB's acoustic data. The tongue shapes and the formant patterns obtained for the 300 simulations were compared to the MRI data and the formant patterns collected from subject PB. For each French extreme vowel, the motor commands providing the best match of the tongue shape experimentally measured on PB in the midsagittal plane and of the corresponding formant patterns have been selected as reference motor commands (Table IV). The corresponding tongue shapes are represented in Fig. 7 (oblique anterior and posterior views) and the formants are given in Table IV (the lip aperture and protrusion are also indicated in this table). Table II summarizes the force levels computed at the end of the selected simulations for every tongue and mouth floor muscle. The values indicated correspond to the algebraic sum of the force levels computed for each

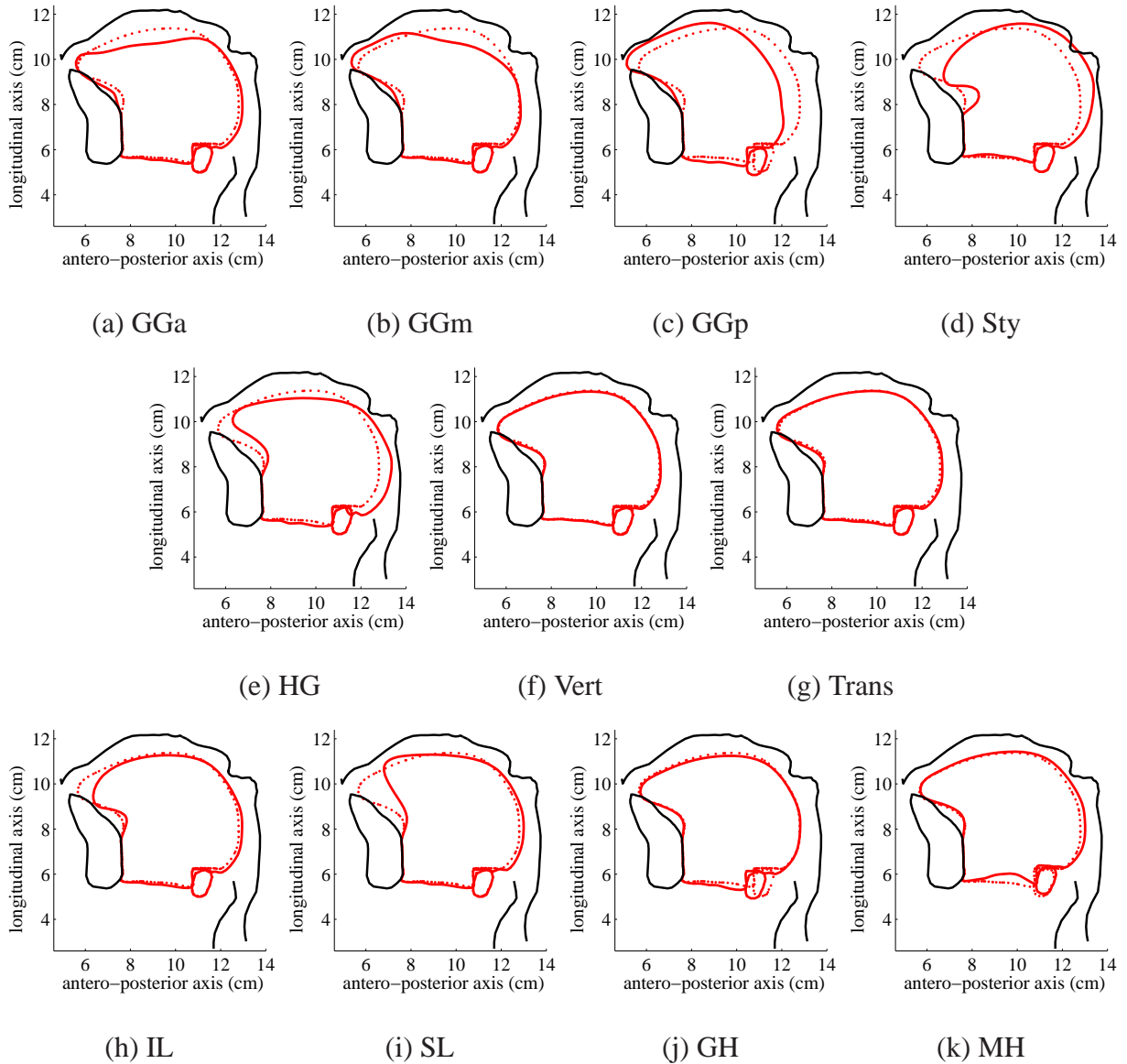


FIG. 5. (color online) Impact of the activation of individual lingual and mouth floor muscles on tongue shape (400 ms command duration, sufficient to reach mechanical equilibrium). The contours of the articulators (tongue and hyoid bone in red, mandible, hard and soft palate, pharyngeal and laryngeal walls in black) are given in the midsagittal plane (tongue tip on the left). For every simulation, the target motor command of the only activated muscle equals 75% of the muscle length at rest, except for the activation of the long muscles Sty, IL and SL (85% of the muscle length at rest). The dotted contours correspond to the tongue shape in its rest position.

macrofiber. It is not a true value of the force exerted on the tongue, but it provides a fair idea of its

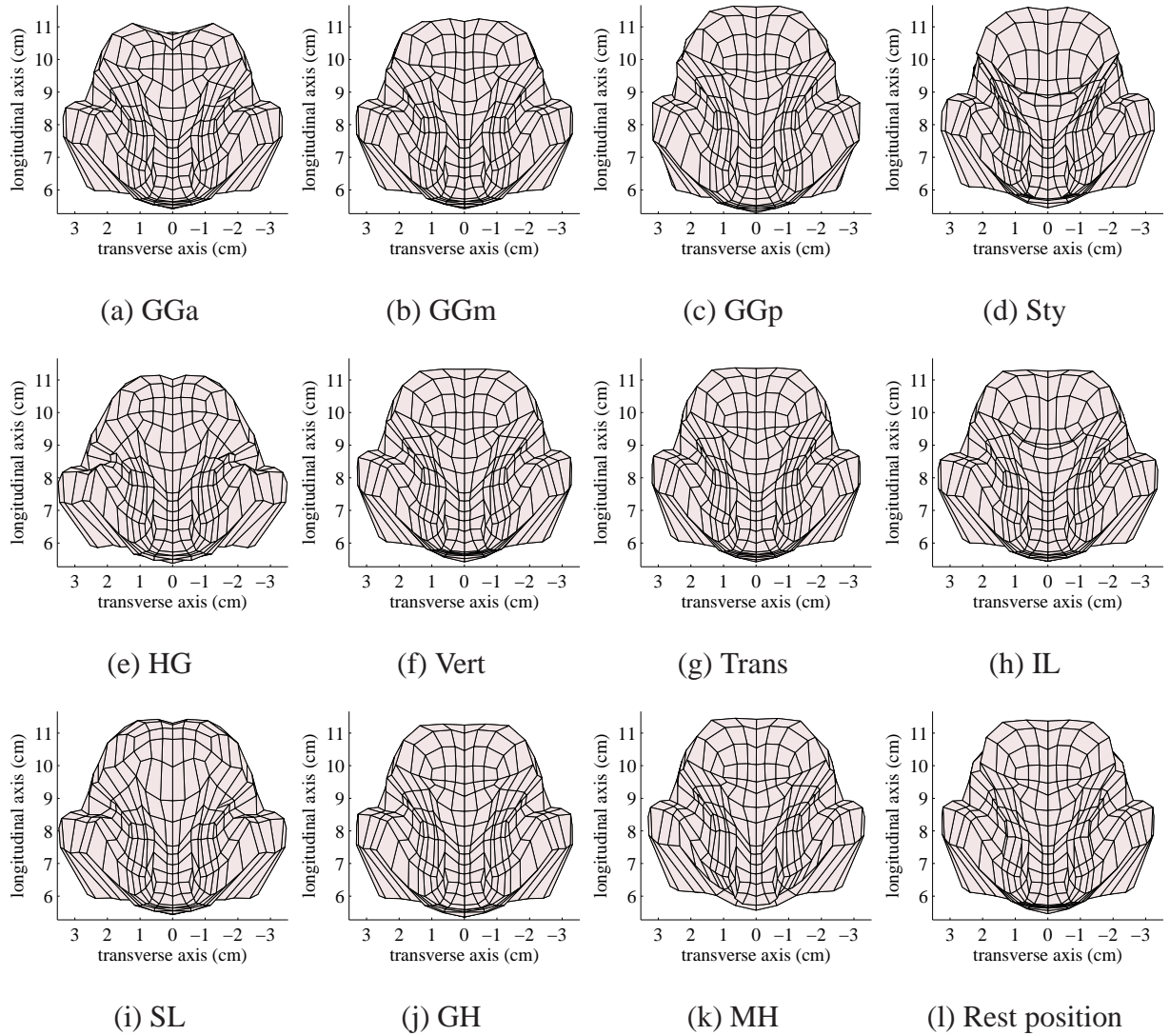


FIG. 6. (color online) Impact of the activation of individual lingual and mouth floor muscles on tongue shape (400 ms command duration, sufficient to reach mechanical equilibrium) [frontal view]. For every simulation, the target motor command of the only activated muscle equals 75% of the muscle length at rest, except for the activation of the long muscles Sty, IL and SL (85% of the muscle length at rest). The shape of the tongue at rest is given for indication on the bottom right.

order of magnitude. Fig. 7 reflects the traditional relationships between the French extreme vowels (anterior vs. posterior, low vs. high) while the formants are consistent with the classic published values and with acoustic data obtained for the speaker PB (Table V). We can note a good corre-



spondence between the formants of the acoustic data measured for PB and those obtained with the simulations. The average difference between the formants that were measured and those that were simulated is below 3.3% for the first four formants. The difference does not exceed 4.3% for the first formant (vowel /u/) and 10.2% for the second formant (vowel /i/).

Due to the redundancy of the system (some pairs of muscles interact as agonist-antagonists), the commands were also chosen such that the amount of force generated by the different muscles remains reasonable. Only the extreme cardinal vowels will be presented in detail.

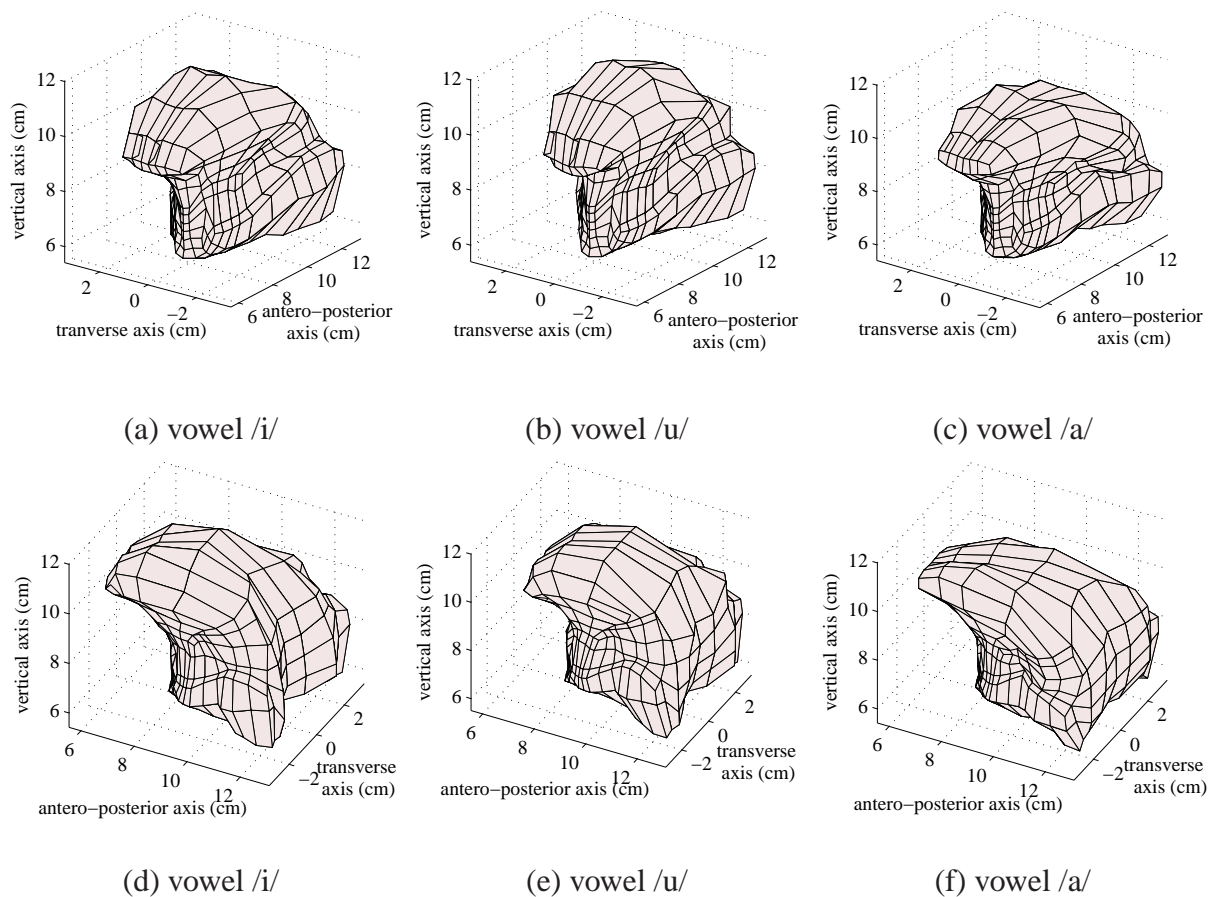


FIG. 7. (color online) Final tongue shape for the simulation of the French cardinal vowels (first row: anterior oblique view, second row: posterior oblique view).

*a. Muscle activation pattern in vowel /i/* Fig. 8 shows the tongue shapes obtained by simulation and those obtained experimentally for the speaker PB (CT data). Some discrepancies can be

seen in the tongue posterior part, but the delimitation of the tongue contours in this area is less precise (the delimitation of the tongue body on CT images is a tedious and less obvious task in this part of the body, due to the presence of the hyoid bone, epiglottis and other soft tissues) and acoustically less relevant than in the anterior part. This figure shows a good correspondence between the experimental results and the computed data, in particular in the anterior part of the tongue, which plays an important role in the production of vowel /i/. As expected from Fig. 5,

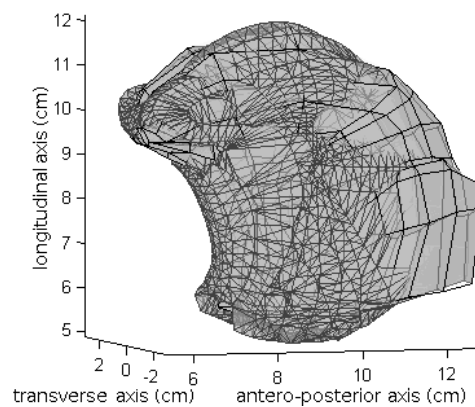


FIG. 8. Superimposition of the shape of the tongue for the speaker PB (CT data) (dense mesh) and the shape of the tongue obtained by simulation (coarse mesh) for vowel /i/.

since vowel /i/ is an anterior and high vowel (Fig. 7(a)), the model predicted the GGp, GH and MH muscles to play a fundamental role in its production. In addition to their slight impact on the tongue geometry (see Section III.A.1), the GH and MH muscles can help stiffen the mouth floor, thanks to a significant propagation of the stress into the lingual tissues. Activated alone, the styloglossus pulls the tongue backwards (Fig. 5(d)); this movement is here counterbalanced by the strong GGp activation, while both muscles elevate the tongue in the palatal region. For the transversalis and the anterior genioglossus, the motor commands ( $\lambda$  commands of the EPH) are larger than the muscle lengths at rest (Table III). From a motor control perspective, these two muscles can consequently be seen as being in their rest state, and their activation is the result of reflex loops (Table II). The transversalis reflex activation avoids an overwidening of the tongue that would otherwise result from the combination of the GGp activation (see Section III.A.1), while ensuring a contact between the palatal arch and the lateral borders of the tongue in the alveolar

region. The GGa reflex activation limits tongue elevation in the median alveolar region, thus creating the slight groove characteristic of an /i/. The voluntary activations are consistent with the EMG data of Baer *et al.* (1988), except for the styloglossus, for which no activity was measured by these authors for vowel /i/. With the model, the combined activation of the GGp and Sty is essential to precisely control the location of the constriction for high vowels. This co-activation is consistent with our previous findings with a 2D tongue model (Payan and Perrier, 1997).

Qualitatively the tongue shape proposed for /i/ is in good agreement with different kinds of data published in the literature. This is true for the 2D shape in the midsagittal plane, which is consistent with Bothorel *et al.* (1986) data for French speech sounds. It is also true for the 3D distribution of the contacts between the hard palate and the upper dental arch on the one side and the tongue lateral borders on the other side. These contacts are represented in Fig. 10(a). The surface of contact stretches over the whole hard palate and is also extended to the inner aspects of the molars. In addition, we can note the presence of contacts between the apex and the mandible inner surface, behind the lower incisors (not shown). These observations are consistent with the electropalatographic data (EPG) of Stone and Lundberg (1996) (Fig. 9) and Yuen *et al.* (2007) for English vowels.

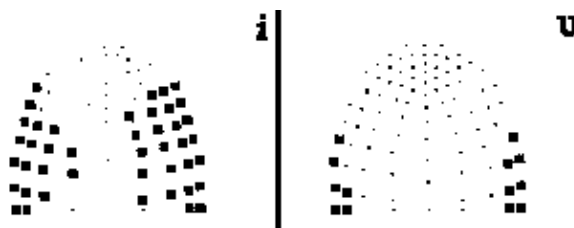


FIG. 9. EPG data for American English vowels /i/ and /u/. Reprinted from Stone, M. and Lundberg, A., J. Acoust. Soc. Am., “Three-dimensional tongue surface shapes of English consonants and vowels”, 99(6), 3728-3737, 1996. Copyright 1996, Acoustical Society of America.

*b. Muscle activation pattern in vowel /u/* The model produces vowel /u/, a posterior and high vowel (Fig. 7(b)), essentially with the activation of the styloglossus, the mylohyoid and the transversalis (Table III). As with vowel /i/, the model requires the activation of the MH to stiffen

the mouth floor and thus contribute to the tongue elevation, due to the complementary action of other muscles. The styloglossus allows the tongue to be pulled both backwards and upwards. The GGp is also active. It increases the size of the vocal tract back cavity by propelling the tongue forward and contributes to the upward movement of the tongue. The transversalis contributes to the limitation of the tongue widening, but this is not its only role. Indeed, for this vowel the model uses an active recruitment of the transversalis in order to facilitate the tongue elevation, due to the incompressibility of the lingual tissues (note, however, that the amount of force generated by the transversalis is close to that used in the production of /i/). The motor commands proposed in our model are consistent with the EMG data of Baer *et al.* (1988). Here again, the 2D tongue shape in the midsagittal plane is in good agreement with Bothorel *et al.* (1986) data. In our simulation, the tongue tip is located in the mid height of the tongue. Figure 10(b) shows the distribution of the contacts of the tongue dorsum and the tongue tip with the surrounding structure, namely the hard and soft palate, the superior dental arch and a part of the pharyngeal walls. The figure shows that the tongue post-dorsal surface is laterally in contact with the inner surface of the molars and, further back, with the lateral sides of the pharyngeal walls. The contacts between the tongue and hard palate observed in the simulations are consistent with the EPG data of Stone and Lundberg (1996) (Fig. 9) and Yuen *et al.* (2007). However, EPG data do not provide information on possible contacts between the tongue and velum.

*c. Muscle activation pattern in vowel /a/* Vowel /a/, a posterior and low vowel, was essentially produced in the model with the activations of the HG and GGa muscles (Fig. 7(c) and Table III). The HG pulls the tongue backward and downward but also rotates the tongue tip toward the palate (Fig. 5(e)). The GGa limits the apex rotation by flattening the tongue tip and maintaining it in contact with the inner surface of the mandible, thus preventing the creation of a sub-lingual cavity, and increasing the size of the anterior cavity. The GGp activation is a reflex activation, since from the motor command point of view it is in its rest state (see Table III); the GGp limits the backward movement of the tongue and thus avoids the occlusion of the vocal tract in the laryngopharyngeal region. The motor commands are in agreement with the EMG data of Baer *et al.* (1988). The

tongue shape in the midsagittal plane is in agreement with Bothorel *et al.*'s (1986) data. The lateral borders of the tongue are in contact with the lower dental arch over its entire length, but not with the palate. The lower surface of the tongue anterior part is partially in contact with the inner surface of the mandible. For vowel /a/, the EPG data of Stone and Lundberg (1996) and Yuen *et al.* (2007) reported an either extremely limited or non-existent contact between tongue and palate; the results obtained are consistent with their data.

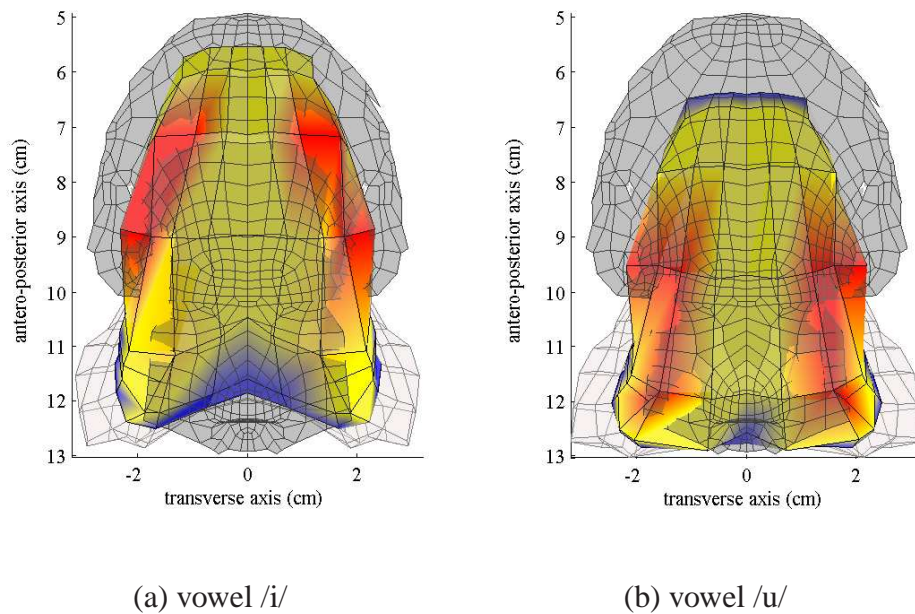


FIG. 10. (color online) Illustration of the contacts between the tongue dorsum and tongue tip, and surrounding structures of the vocal tract for vowels /i/ (a) and /u/ (b) (superior view, apex at the top). The surrounding structures, represented by translucent gray meshes, include the hard palate, the upper dental arch, the velum and the pharyngeal walls close to the velum. The entire tongue mesh is represented, but only the tongue surface elements used for the detection of potential contacts between the tongue and the surfaces listed above are colored. Red elements represent tongue surfaces in contact with the surrounding structures, yellow elements represent tongue surfaces close to the surrounding structures, and blue elements represent tongue surfaces far from the surrounding structures.

## **B. Highlighting the role of the transverse muscle in midsagittal tongue shaping**

A 3D biomechanical tongue model allows the study of the transverse muscle action during speech production. Since speech has experimentally mainly been studied in the sagittal domain, the potential role of this muscle has essentially been ignored. However, it could be of great importance in speech production, since it is the only muscle able to directly act on tongue deformations in the transverse dimension orthogonal to the sagittal plane.

The role of the transverse muscle in the midsagittal deformation of the tongue was recently observed by Gilbert *et al.* (2007) for swallowing through the analysis of diffusion-weighted MRI measurements. They found in particular that the recruitment of the transversalis is used to generate depressions in the tongue to facilitate the movement of the food toward the pharynx. Unfortunately, similar experimental observations do not yet exist for speech, and it is a strength of our 3D model that it offers the possibility to quantitatively assess the role of the transversalis in speech production. As a matter of fact, the simulations of vowel production reported in the preceding sections highlighted the fundamental role of this muscle in the maintenance of the tongue dimension along the transverse direction and its influence on midsagittal shaping. These results have been obtained in the context of our motor control model, based on the EPH theory, which gives an account of the postural control in a particularly effective way, thanks to the integration of reflex activation in the muscle force generation mechanisms. Indeed, the model predicts that for vowel /i/ (and also for the high anterior vowels /y/ and /e/ not presented here), the transverse muscle is active, despite the fact that the motor commands for this muscle were those of the rest position or higher (see Eq. 2). This is the result of a reflex activation (or limited active contraction) due to the lengthening of the transverse fibers induced by the centrally activated muscles that mainly act on the tongue shape in the sagittal plane. This reflex activation limits the amplitude of the deformations in the transverse dimension and, in turn, due to the incompressibility of tongue tissues, it increases the deformations in the sagittal plane. According to the simulations, a voluntary activation of the transversalis would lead to a decrease in the tongue width that does not seem compatible with the production of high anterior vowels, unless this decrease can be compensated by

the action of other muscles. Hence, the combination of a voluntary co-activation of the transversalis and of other tongue muscles could also be considered as an alternative to the proposed reflex activation of the transversalis. Such a strategy is realistic, but it would imply the activation of a larger number of muscles acting antagonistically; inducing an increase the amount of force necessary to produce high anterior vowels. Our simulations do not rule out the possibility of a voluntary activation of the transversalis. However, such a strategy does not sound like an economical way to control tongue shapes for high vowels. As already mentioned above, 2D or 2.5D models, such as those of Payan and Perrier (1997) or Dang and Honda (2004), could only account for tongue incompressibility in the sagittal plane due to a simplifying assumption assimilating volume conservation and area preservation in this very plane. In a way, this simplifying approach implicitly included the role of the transverse muscle, without formalizing it in explicit terms. We have seen in Section III.A.1 that this hypothesis led to partially inaccurate conclusions concerning the role of muscles taken individually. Our 3D modeling approach allows these former conclusions to be corrected and emphasizes the indirect role of the transverse muscle in the shaping of the tongue midsagittally (Fig. 7(a)).

Based on simulations made with their 2D model, Perrier *et al.* (2000) concluded that the main directions of deformation for the tongue during speech production as observed for different languages (namely the factors front and back raising of the PARAFAC analysis of Harshman *et al.* (1977), see Jackson (1988); Maeda (1990); Nix *et al.* (1996); Hoole (1998), or more recently Mokhtari *et al.* (2007)) did not result from a specific speech control, but emerged naturally from the actions of the major tongue muscles (GGp, GGa, HG and Sty). Similar conclusions could be drawn from Honda's (1996) EMG data. The results concerning the role of individual muscles in our 3D model can be used to reformulate these conclusions more accurately. The main directions of deformation could indeed emerge naturally, provided that the tongue widening along the transverse direction is strictly controlled by the reflex transversalis activation. This reflex activation, based on the use of the motor commands at rest, is not likely to be speech-specific, since it allows the tongue to remain within the space determined by the dental arches, possibly in order to avoid biting problems (several observations indeed show a widening of the tongue for edentulous people

(Kapur and Soman, 1964)). Taking into account this reflex limitation of tongue width seems to be essential to understanding the precise control process of the place of articulation in the vocal tract.

#### **IV. VARIABILITY OF MOTOR COMMANDS AND TONGUE POSITIONING**

##### **ACCURACY FOR VOWEL /i/**

###### **A. Methodology**

The accuracy of speech motor control is an important and still unsolved issue. Indeed, speech movements can be as short as a few tens of milliseconds, so that it is traditionally suggested that cortical feedback, involving long latency loops, can only be used to monitor speech after its production and not during on-going production (see for example Perkell *et al.* (2000) for details). Tongue positioning has to be very accurate though for the production of some sounds, such as fricatives and high vowels. This apparent contradiction (the absence of cortical feedback versus the accuracy requirement) suggests that speech motor control has developed into a very efficient process to ensure, in a simple way, accuracy and stability of tongue positioning. This efficient treatment and accuracy can be seen as the result of the high amount of training and experience in speaking that speakers have.

For the high vowel /i/ more specifically, it has been argued that control accuracy would come from a combination of biomechanical effects, namely the co-contraction of the GGp and the GGa associated with tongue/palate contacts (Fujimura and Kakita, 1979). This effect is called the “saturation effect”. Using a rudimentary 3D tongue model, Fujimura and Kakita (1979) showed that the tongue was stabilized during the production of /i/ when laterally pressed against the palate, due to the combined action of the GGa and GGp, which stiffened the tongue. Our 3D model, which integrates numerous improvements as compared to Fujimura and Kakita’ (1979) original model (smaller mesh elements, non-linear tissue elasticity, gravity, stiffening due to activation, accurate model of contacts), offers a powerful context to revisit this hypothesis and to better understand how the different biomechanical factors interact. With the current model, a number of simulations were realized around the reference tongue shape for /i/ to evaluate the articulatory and acoustic



sensitivity of the vowel to changes provided to the motor commands. The tongue shape variations as well as the formant variations resulting from small changes in the central commands were studied for this vowel, so as to better understand the patterns of variability observed during its production. The motor commands defined previously (cf. Section III and Table III) formed the basis of this study. The motor commands of the main tongue muscles (i.e. the anterior, medial and posterior genioglossus, the styloglossus, the hyoglossus, the transversalis, the lingual inferior and superior muscles and the mylohyoid) were independently modified. For the GGa, GGp, Sty, MH and Trans, the motor commands were modified by  $\pm 2\%$ ,  $\pm 5\%$ ,  $\pm 8\%$  and  $\pm 10\%$  around their values at target. For the GGm, HG, IL and SL, which were not active during the production of vowel /i/ in our modeling, the motor commands were only modified by  $-2\%$ ,  $-5\%$ ,  $-8\%$  and  $-10\%$ , since an increase in their values would let them inactive. The same lip protrusion and aperture parameters as previously applied were used to generate the acoustic signals and to determine the formants associated with the different area functions. Table VI indicates the first three formants for each of the 56 simulations.

## B. Results

Fig. 11 shows the scatter plots in the midsagittal plane for 6 nodes on the tongue surface obtained from the simulations. Results are presented in the upper left panel for the variations of all muscle commands together, and in the other panels, more specifically, for the variations of the commands to three muscles that play a major role in the production of vowel /i/: the styloglossus and the anterior and posterior genioglossus. For the global results (upper left panel),  $3\sigma$  ellipses characterizing the node position dispersion with a Gaussian statistical model are superimposed on the data. Considering first the influence of all muscles taken together, the following observations can be made. In the pharyngeal and velopharyngeal regions (three most posterior nodes), the major axes of the dispersion ellipses essentially correspond to a displacement along the front-to-back direction (from the pharyngeal to the velopharyngeal position, length of the major axes 3.0, 3.9 and 4.4 mm, respectively, length of the small axes 1.5, 1.4, 0.8 mm, angles of the major axes

with the antero-posterior axis 133, 147, 173 degrees). In the palatal and alveopalatal parts of the tongue (second and third nodes from the front), the ellipses have no clear direction and they tend to be more circular. In addition, the maximal variability is smaller than in the back part of the tongue (length of the major axes 2.9 and 3.5 mm, respectively, length of the small axes 2.4 and 2.1 mm). Finally, in the apical part (most anterior node) a very strong correlation is observed between elevation and forward movement. This leads to a global ellipsis orientation similar to the one observed in the tongue blade region, but much stronger and clearer and with much more variation along the principal axis (length of the major axis 8.3 mm, length of the small axis 3.4 mm, angle of the major axis 147 degrees).

These observations are in quite good agreement with experimental data published in the literature about vowel variability. See, in particular, Perkell and Nelson (1985), Beckman *et al.* (1995), or Mooshammer *et al.* (2004): the front-back orientation of the variability in the velar region and the reduced variability in the palatal and alveopalatal regions (the region of constriction for /i/) were already observed by these authors. In addition, the absence of clear orientation of the ellipses in the region of constriction was also observed in 2 of the 3 subjects studied by Mooshammer *et al.* while Perkell and Nelson and Beckman *et al.* rather observed ellipses parallel to the palatal contour in this region. The large variability in the apical part was observed by Mooshammer *et al.*, but not by Perkell and Nelson and Beckman *et al.*. Note, however, that this specific aspect of the displacement of the apex relative to that of the tongue body has already been observed many times by different authors, in particular Perkell (1969).

Our model allows one to look more specifically at the biomechanical factors influencing these articulatory patterns. Looking at the variability associated with the variation in the GGa, GGp, and Sty activations separately, it can be observed that the angle of the main ellipses in the three posterior nodes is similar to the orientation of the scatter plots generated by the Sty and GGa. However, for the GGp, the largest variability is also observed in the front-back direction. The reduction in the variability in the region of constriction is observed both for the Sty and the GGp, while the GGa, in contrast, shows the largest variability in this region. This can be interpreted in the light of the palatal contacts for vowel /i/ (see Fig. 10). The GGp and Sty act on the position

of the whole tongue body, whose variability in the constriction region is limited by the palatal contacts. The GGa influences only the center of the front part of the tongue, which is not in contact with the palate. It can be noted that in our simulations the styloglossus generates the largest variability, as compared to the other muscles, except as explained above in the constriction region. This phenomenon is intrinsically linked to the approach that was used in our simulations. In the context of the  $\lambda$ -model, since the styloglossus macrofibers are longer than in the other muscles, a given percentage of variation generated a larger change in the commands for the styloglossus, and then, in turn, larger changes in force level. This approach could have influenced the global amount of variability depicted in the upper left panel of Fig. 11, but not its relation with the node position on the tongue, neither in terms of orientation nor of amplitude, except for the tongue tip variation, which is largely dependent on the styloglossus.

As concerns the other muscles (not depicted in Fig. 11), their impacts are smaller, but some interesting observations can be mentioned. The transversalis shows a notable contribution in the variability in the velopharyngeal region (third node from the back), where an increase in its activation induces backward displacements of the tongue dorsum. The mylohyoid participates in the up-down displacements, with an amplitude of approximately 1.5 mm in the pharyngeal region.

### **C. The saturation effect for vowel /i/ revisited**

From the simulations of the consequences of motor command variability for tongue shape for vowel /i/, interesting conclusions can be drawn for this vowel concerning the influence of the GGa and of its variability on the vocal tract shape and formants. Contrary to what could be inferred from the statistical processing of articulatory speech data (see for example Badin *et al.*, 2002), the central tongue groove observed for vowel /i/ in many languages does not seem to be a consequence of the combined activations of the GGp and Sty muscles. It is in fact obtained in our model very specifically by activating the GGa. As mentioned above, this statement is consistent with Fujimura and Kakita (1979)'s hypothesis of a co-activation of the GGp and GGa in the production of /i/.

However, the variability patterns generated with our model, together with their interpretation

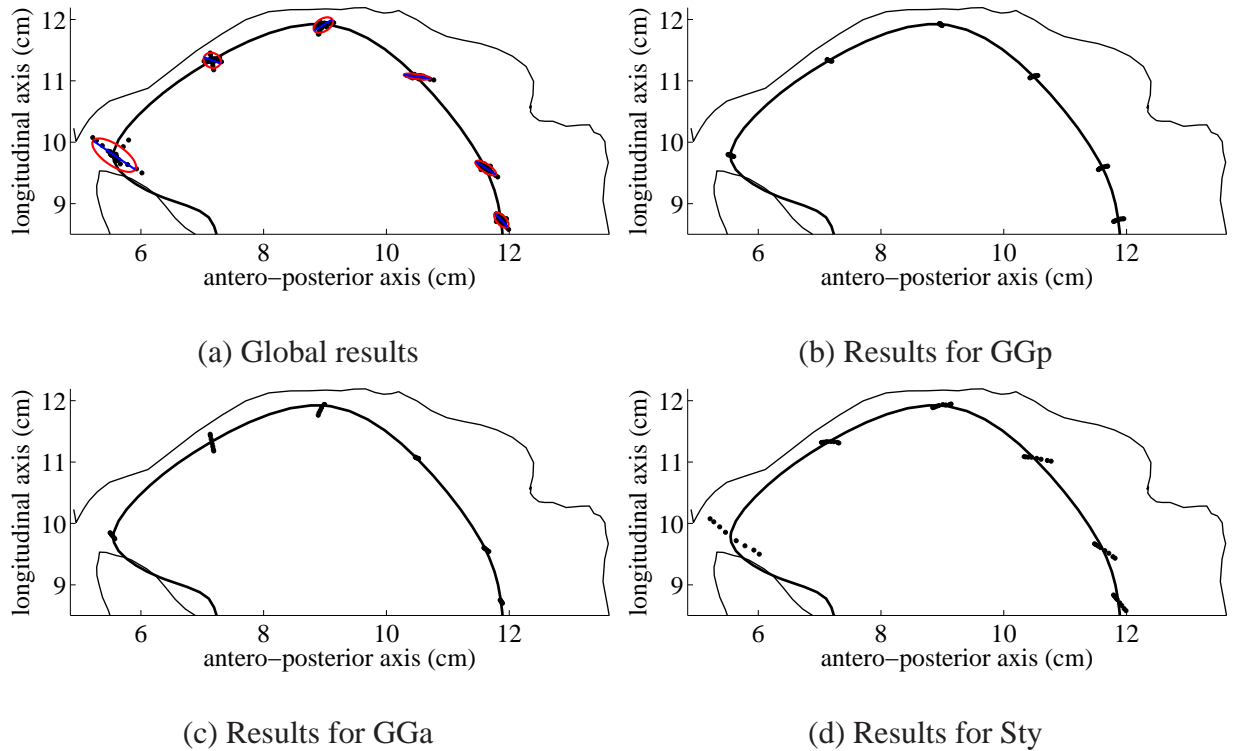


FIG. 11. (color online) Displacement scatter plots (black circles) for vowel /i/ in the midsagittal plane. Only the surface of the tongue is represented. Panel (a) summarizes the results obtained for the 9 muscles whose motor commands were modified. The  $3\sigma$  ellipses of dispersion (red) are also represented, and their major axes are drawn in blue. Panels (b-d) represent the dispersion obtained when modifying the motor commands of the posterior genioglossus (b), the anterior genioglossus (c) and the styloglossus (d) only.

in terms of the respective influence of each muscle, strongly suggest that there is no saturation effect, which would facilitate the accurate control of the constriction area for /i/. This observation questions Fujimura and Kakita's original hypothesis as well as the numerous follow-up contributions that have used this hypothesis to explain the control of high front vowels, in particular those of Perkell *et al.* (2000) and Badin *et al.* (1990).

In agreement with the work of the previous authors, our model tends to confirm that the tongue is indeed stabilized in its entirety by these palatal contacts, and that this should contribute to simplifying its motor control. However, in contrast to Fujimura and Kakita's tongue model, which was quite rudimentary because of the computational limitations existing at that time, our model

shows that the variability of the GGa activation leads to a variation in the alveolar groove with noticeable consequences for its formant pattern (see below). This variation is highly localized in the globally well-stabilized tongue, but it is fundamental to acoustics, because it plays on the constriction size.

The amplitudes of variation for the first three formants were as follows:  $\Delta F1 \approx 103$  Hz,  $\Delta F2 \approx 250$  Hz,  $\Delta F3 \approx 283$  Hz<sup>2</sup> (Table VI). An important part of the variability is due to the styloglossus (impact on F1, F2 and F3, but see our remark above about the force level variation for this muscle), but other muscles also have a noticeable influence, either on the first, second or third formant. The F1 variability is due in great part to the modifications in the level of activation of the GGa and Sty, and secondarily of the GGp and SL. According to the model, the variability of F2 results mainly from the modification of the Sty and GGm motor commands, while that of F3 is due to the Sty and Trans.

The variability of F1 for /i/ has important consequences; indeed the perception of vowel /i/ is sensitive to F1 variations in French (one can easily move from /i/ to /e/). Likewise for F3, too low an F3 value moves the perception from /i/ to /y/ (Schwartz and Escudier, 1987). It can therefore be concluded that the articulatory variability generated in the simulations is too important to ensure proper perception of vowel /i/. It is necessary to reduce it. This need for an active reduction of the articulatory variability is consistent with the observations made by Mooshammer *et al.* (2004) with German speakers: they concluded from their study that the potential saturation effect related to the interaction between tongue and palate did not seem to be sufficient for their speakers to meet the perceptive requirements of the German vowel system, and that a specific control adapted to the individual palate shape of each speaker was necessary to limit the articulatory variability and its consequences for perception.

This is then quite an important result as it throws back into question a widely made assumption to explain the precise control of the vowel /i/, namely the saturation effect.

## V. IMPACT OF GRAVITY ON LINGUAL MOVEMENTS

With the increasing use of MRI systems, numerous speech data are acquired while the subject is lying on his or her back. Due to the change in the orientation of gravitational forces in relation to the head, this position is likely to alter the vocal tract shape and its control. This is why many studies have tried to compare the production of speech sounds and speech articulations (either vowels or consonants) for subjects when they are sitting, standing or lying (Weir *et al.*, 1993; Tiede *et al.*, 2000; Shiller *et al.*, 2001; Stone *et al.*, 2007). Our model allows the impact of gravity to be tested and quantitatively assessed. With this aim in view, the pattern of activation needed to keep the tongue in its neutral position was first studied in the presence of a gravitational field in an upright and in a supine position. Then, the influence of gravity on the tongue shape during the production of vowels was evaluated together with its impact on the acoustic signal.

### A. Impact of gravity in the absence of active and reflex muscle activation

First, the impact of gravity alone on the tongue shape and position was studied: the force generator was deactivated (no internal force could be generated, whether active or reflex forces). The final tongue shape is given in Fig. 12 for an upright and supine position starting from the rest position and after a 1 s movement. For a standing subject, there is a clear lowering of the tongue body, which is particularly marked in the posterior radical part of the tongue, but is also visible in its apical region (approximately 1.5 mm). For a lying subject, the gravity alone produces a strong backward displacement of the tongue body, with a displacement of the tongue tip equal to 9 mm. These results show that tongue muscle activations are required to maintain the tongue in its rest position, whether the subject is lying on his back or standing.

Reflex activation obtained with motor commands equal to muscle lengths at rest is not sufficient to maintain the tongue in the rest position, as shown by Fig. 13 for a 1 s simulation. A small backward displacement of the apex ( $\approx 1$  mm) and of the rear part of the tongue is visible in the upright position, as well as a more limited rotation of the apex in the supine position than in the absence of muscle activations (displacement of the tongue tip  $\approx 3$  mm). A limited voluntary

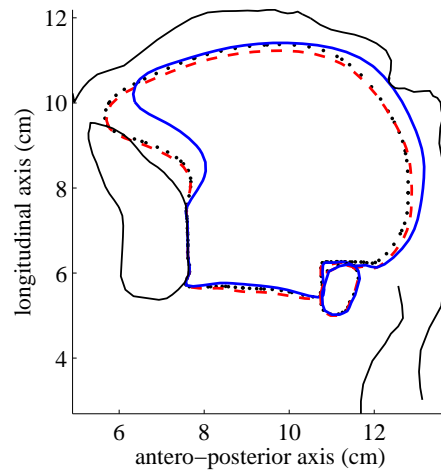


FIG. 12. (color online) Final tongue position in the midsagittal plane for 1 s simulation under the influence of gravity alone. The neutral position of the tongue and the hyoid bone (rest position for a subject in upright position) is represented by a black dotted line, the final shape for the tongue and hyoid bone for a subject in upright position by a red dashed line, and for a subject in supine position by a blue solid line. The black solid lines correspond to the contours of the mandible, hard and soft palate, and pharyngeal and laryngeal walls.

activation of the GGp and GGa combined with a stronger activation of the MH associated with the reflex activation of the other tongue and mouth floor muscles can compensate for the gravity effect (commands indicated in Table III for vowel /ə/). Based on the model, the MH activation strengthens the mouth floor and limits the lowering of the tongue inferior region (Fig. 5(k)). The GGp action prevents the backward displacement of the tongue (Fig. 5(c)) and the GGa counteracts the GGp action in the apical and dorsal areas, limiting the tongue elevation (Fig. 5(a)). A good equilibrium between the activation of these three muscles, based on numerous simulations, leads to the stabilization of the tongue in a “neutral” upright position. Corresponding force levels computed at the end of the simulation for every tongue and mouth floor muscle are given in Table II (vowel /ə/).

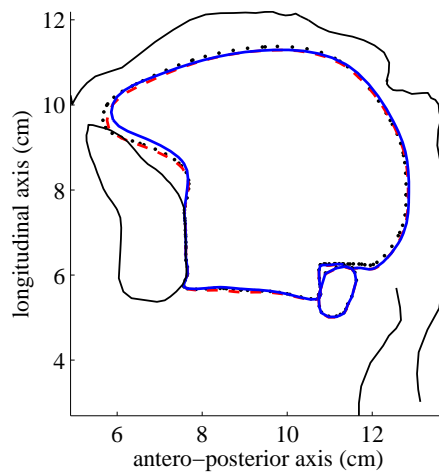


FIG. 13. (color online) Final tongue position in the midsagittal plane for 1 s simulation under the influence of the reflex activation alone. The neutral position of the tongue and the hyoid bone (rest position for a subject in upright position) is represented by a black dotted line, the final shape for the tongue and hyoid bone for a subject in upright position by a red dashed line, and for a subject in supine position by a blue solid line. The black solid lines correspond to the contours of the mandible, hard and soft palate, and pharyngeal and laryngeal walls.

## B. Impact of gravity on French oral vowels

The impact of the subject position (upright or supine) on vowel production was studied by modifying the orientation of the gravitational field. Simulations were realized for the supine position for the 10 French oral vowels with the same commands and the same timing as in the upright position. The tongue shapes and positions for the supine and upright positions were compared, as well as the force levels for tongue and mouth floor muscles.

The differences in tongue shape and formant values between upright and supine positions were negligible for all vowels. However, differences were noticed in the level of forces developed by the GGp, with an increase in supine position that is variable across vowels: the peak and the final forces increased on the order of 8% for /a/, 7% for /u/ and 1% for /i/. On the whole, this modification in the force level affects in percentage more posterior than anterior vowels. This is consistent with the fact that the production of front vowels necessitates a strong force from the



GGp anyway, in comparison to which the gravitational force becomes quasi negligible. Our results are also in agreement with experimental observations, in which an increase in the GGp activity in supine position is commonly observed (see for example the EMG data of Niimi *et al.* (1994) and Otsuka *et al.* (2000)).

In the model, the tongue weight, which is on the order of one Newton, is small as compared to the muscular forces. Hence, feedback activation efficiently counteracts the effects of gravity orientation changes, and limits tongue shape variation. This small shape variation is in contradiction to experimental values typically found in the literature. For instance, Badin *et al.* (2002) reported a more important backward displacement of the tongue for both vowels and consonants in supine position (MR images) compared to upright position (cineradiofilm images), which they attributed to the tongue weight. Shiller *et al.* (1999) found differences in the formant values between the upright and supine position for vowels /a/ and /ε/. They found that, when the head was in the supine orientation, the jaw was rotated away from occlusion, which led them to conclude that the nervous system did not completely compensate for changes in head orientation relative to gravity. In the current model, the fact that the model has a fixed jaw position (the same for the supine and upright orientation) could in part explain the absence of notable differences. However, it should be mentioned that recent experimental findings provide good support for our simulation results. Indeed, Stone *et al.* (2007) showed that the impact of gravity was low (or even negligible) for some speakers when vowels were pronounced in context and not in an isolated manner as has thus far been the case.

## VI. CONCLUSION

A 3D finite element model of the tongue has been presented which was used to study biomechanical aspects and tongue control during vowel production. The model provides a high level of realism both in terms of compliance with anatomical and morphological characteristics of the tongue and in terms of soft tissue modeling hypotheses (geometrical and mechanical non-linearity). The tongue and mouth floor muscles were controlled using a force generator based on

the EPH theory. Simulations with the model coupled with an acoustic analog of the vocal tract allowed muscle activation patterns to be proposed for the French oral vowels which were consistent with the EMG data published in the literature and which generated realistic tongue shapes, tongue/palate contact patterns and formant values. The simultaneous analysis of these activation patterns and of the actual muscle forces generated for each vowel revealed, among other things, a systematic feedback activation of the transversalis. This suggests that this muscle is used to maintain the dimension of the tongue quasi-constant along the transverse direction orthogonal to the sagittal plane. This role is very important for the control of tongue shape in the midsagittal plane, since, due to tongue tissue incompressibility, it allows more deformation in this plane. This is consistent with the recent experimental observations made by Gilbert *et al.* (2007) for swallowing. The results obtained from the simulations have led us to conclude that the main directions of tongue deformation in the midsagittal plane (as described by the classic front and back raising factors of Harshman *et al.* (1977)) could naturally emerge from the combined action of the major tongue muscles and of the transversalis playing the role of a “size maintainer” in the transverse direction. This conclusion is in line with Perrier *et al.* (2000), who suggested that these main directions of deformation are not speech specific, but are intrinsically linked to tongue muscle arrangements.

The muscle activation patterns proposed for each French vowel served as a basis for further studies. The patterns of articulatory variability, and their associated acoustic variability, were analyzed for local changes in the central commands for vowel /i/. These results cast doubt over the idea, generally accepted since the work of Fujimura and Kakita (1979), that a muscular saturation due to a simultaneous co-activation of the GGa and GGp muscles would facilitate the accurate control of /i/. Indeed, the tongue grooving in the constriction region was shown to be sensitive to change in the GGa activation with a significant impact on the F1 formant value. The impact of gravity was also considered. Simulations showed the importance of low-level feedback in the postural control for the rest position, as well as the impact of the head orientation on the tongue shape and position. These results are at odds with data published in the literature for isolated sound production, but they find support in the recent work of Stone *et al.* (2007) on the production

of vowels in context.

Further work will be required to significantly reduce the computation time, and thus increase the number of simulations and refine the results. Studies have also been undertaken to assess the contribution of this model to medical applications, in particular the surgical planning of tongue exeresis, with lingual tissue resection and reconstruction processes. First results have proved to be promising and show the potential of such a model (Buchillard *et al.*, 2007). The results obtained for the planning of tongue surgeries and the comparison with patients' data should also provide particularly interesting information about the compensation processes and the motor control mechanisms.

## **Acknowledgments**

The authors wish to thank Ian Stavness for helpful comments and suggestions. This project was supported in part by the EMERGENCE Program of the Région Rhône-Alpes and by the P2R Program funded by the CNRS and the French Foreign Office (POPAART Project).

## **Endnotes**

1. Program written by Pierre Badin (ICP/GIPSA-lab)
2. It should be noted that these values were obtained with tongue motions starting from a resting state. Modifying this starting state would have an impact on the formant values, but due to the simulation durations, sufficient to reach an equilibrium position, and to the model of motor control, the variations of the formant values should remain limited.

## **References**

Abry, C., Boë, L.-J., Corsi, P., Descout, R., Gentil, M., and Graillot, P. (1980), *Labialité et phonétique : données fondamentales et études expérimentales sur la géométrie et la motricité*

*labiales (Labiality and phonetics: fundamental data and experimental studies on lip geometry and mobility)* (Publications de l'Université des langues et lettres de Grenoble).

Badin, P., Bailly, G., Revéret, L., Baciú, M., Segebarth, C., and Savariaux, C. (2002), "Three-dimensional linear articulatory modeling of tongue, lips and face, based on MRI and video images," *J. Phonetics* **30**(3), 533–553.

Badin, P., Perrier, P., Boë, L.-J., and Abry, C. (1990), "Vocalic nomograms: Acoustic and articulatory considerations upon formant convergence," *J. Acoust. Soc. Am.* **87**(3), 1290–1300.

Baer, T., Alfonso, P. J., and Honda, K. (1988), "Electromyography of the tongue muscles during vowels in /əpVp/ environment," *Ann. Bull. RILP* **22**, 7–19, URL <http://www.umin.ac.jp/memorial/rilp-tokyo/>.

Bathe, K.-J. (1995), *Finite Element Procedures* (Prentice Hall, Englewood Cliffs, New Jersey), second ed.

Beckman, M. E., Jung, T.-P., Lee, S.-L., de Jong, K., Krishnamurthy, A. K., Ahalt, S. C., Cohen, K. B., and Collins, M. J. (1995), "Variability in the production of quantal vowels revisited," *J. Acoust. Soc. Am.* **97**(1), 471–490.

Boë, L.-J., Granat, J., Autesserre, D., Perrier, P., and Peyre, É. (2006), "Variation et prédiction de la position de l'os hyoïde de l'Homme moderne (Variation and prediction of the hyoid bone position for modern man)," *Biom. Hum. Anthropol.* **24**(3–4), 257–272.

Bothorel, A., Simon, P., Wioland, F., and Zerling, J.-P. (1986), *Cinéradiographie des voyelles et des consonnes du français (Cineradiography of vowels and consonants in French)* (Institut de Phonétique, Université Marc Bloch, Strasbourg, France).

Buchaillard, S., Brix, M., Perrier, P., and Payan, Y. (2007), "Simulations of the consequences of tongue surgery on tongue mobility: Implications for speech production in post-surgery conditions," *Int. J. Med. Robot. Comp.* **3**(3), 252–261.

Buchaillard, S., Perrier, P., and Payan, Y. (2006), "A 3D biomechanical vocal tract model to study speech production control: How to take into account the gravity?" in *Proceedings of the 7th International Seminar on Speech Production* (Ubatuba, Brazil), pp. 403–410.

Dang, J. and Honda, K. (2004), "Construction and control of a physiological articulatory model,"

- J. Acoust. Soc. Am. **115**(2), 853–870.
- Duck, F. A. (1990), *Physical Properties of Tissues: A Comprehensive Reference Book* (Academic Press, London, UK).
- Fang, Q., Fujita, S., Lu, X., and Dang, J. (2008), “A model based investigation of activation patterns of the tongue muscles for vowel production,” in *Proceedings of InterSpeech 2008* (Brisbane, Australia), pp. 2298–2301.
- Feldman, A. G. (1986), “Once more on the equilibrium-point hypothesis ( $\lambda$  model) for motor control,” J. Mot. Behav. **18**(1), 17–54.
- Feldman, A. G. and Latash, M. L. (2005), “Testing hypotheses and the advancement of science: recent attempts to falsify the equilibrium point hypothesis.” Exp. Brain. Res. **161**(1), 91–103.
- Fujimura, O. and Kakita, Y. (1979), “Remarks on quantitative description of lingual articulation,” in *Frontiers of Speech Communication Research*, edited by B. Lindblom and S. Öhman (Academic Press, San Diego), pp. 17–24.
- Gérard, J.-M., Ohayon, J., Luboz, V., Perrier, P., and Payan, Y. (2005), “Non-linear elastic properties of the lingual and facial tissues assessed by indentation technique. Application to the biomechanics of speech production,” Med. Eng. Phys. **27**(10), 884–892.
- Gérard, J.-M., Perrier, P., and Payan, Y. (2006), “3D biomechanical tongue modelling to study speech production,” in *Speech Production: Models, Phonetic Processes, and Techniques*, edited by J. Harrington and M. Tabain (Psychology Press, New-York, USA), pp. 85–102.
- Gérard, J.-M., Wilhelms-Tricarico, R., Perrier, P., and Payan, Y. (2003), “A 3D dynamical biomechanical tongue model to study speech motor control,” Recent Res. Dev. Biomech. **1**, 49–64.
- Gilbert, R. J., Napadow, V. J., Gage, T. A., and Wedeen, V. J. (2007), “Anatomical basis of lingual hydrostatic deformation,” J. Exp. Biol. **210**, 4069–4082.
- Gomi, H. and Kawato, M. (1996), “Equilibrium-point control hypothesis examined by measured arm-stiffness during multi-joint movement,” Science **272**(5258), 117–120.
- Gribble, P. L. and Ostry, D. J. (1999), “Compensation for interaction torques during single- and multijoint limb movement,” J. Neurophysiol. **82**, 2310–2326.
- Harshman, R., Ladefoged, P., and Goldstein, L. (1977), “Factor analysis of tongue shapes,” J.

- Acoust. Soc. Am. **62**(3), 693–713.
- Hashimoto, K. and Suga, S. (1986), “Estimation of the muscular tensions of the human tongue by using a three-dimensional model of the tongue,” *J. Acoustic Soc. Japan* **7**(1), 39–46.
- Hinder, M. R. and Milner, T. E. (2003), “The case for an internal dynamics model versus equilibrium point control in human movement,” *J. Physiol.* **549**, 953–963.
- Honda, K. (1996), “The organization of tongue articulation for vowels,” *J. Phonetics* **24**(1), 39–52.
- Hoole, P. (1998), “Modelling tongue configuration in German vowel production,” in *Proceedings of the 5th International Conference on Spoken Language and Processing* (Sidney, Australia), vol. 5, pp. 1867–1870.
- Huxley, A. F. (1957), “Muscle structure and theories of contraction,” *Prog. Biophys. Chem.* **7**, 255–318.
- Ito, T., Murano, E. Z., and Gomi, H. (2004), “Fast force-generation dynamics of human articulatory muscles,” *J. Appl. Physiol.* **96**(6), 2318–2324.
- Jackson, M. T. (1988), “Analysis of tongue positions: language-specific and cross-linguistic models,” *J. Acoust. Soc. Am.* **84**(1), 124–143.
- Kakita, Y., Fujimura, O., and Honda, K. (1985), “Computation of mapping from muscular contraction patterns to formant patterns in vowel space,” in *Phonetic Linguistics*, edited by V. A. Fromkin (Academic, Orlando, FL), pp. 133–144.
- Kapur, K. K. and Soman, S. D. (1964), “Masticatory performance and efficiency in denture wearers,” *J. Prosthet. Dent.* **14**(4), 687–694.
- Laboissière, R., Ostry, D. J., and Feldman, A. G. (1996), “The Control of Multi-Muscle Systems: Human Jaw and Hyoid Movements,” *Biol. Cybern.* **74**, 373–384.
- Maeda, S. (1990), “Compensatory articulation during speech: evidence from the analysis and synthesis of vocal-tract shapes using an articulatory model,” in *Speech Production and Speech Modeling*, edited by W. J. Hardcastle and A. Marchal (Kluwer Academic Publishers), pp. 131–149.
- Miyawaki, K., Hirose, H., Ushijima, T., and Sawashima, M. (1975), “A Preliminary Report on the Electromyographic Study of the Activity of Lingual Muscles,” *Ann. Bull. RILP* **9**, 91–106, URL

<http://www.umin.ac.jp/memorial/rilp-tokyo/>.

Mokhtari, P., Kitamura, T., Takemoto, H., and Honda, K. (2007), “Principal components of vocal-tract area functions and inversion of vowels by linear regression of cepstrum coefficients,” *J. Phonetics* **35**(1), 20–39.

Mooshammer, C., Perrier, P., Fuchs, S., Geng, C., and Pape, D. (2004), “An EMMA and EPG study on token-to-token variability,” *AIPUK* **36**, 47–63.

Mooshammer, C., Perrier, P., Fuchs, S., Geng, C., and Payan, Y. (2001), “The Control of Token-to-Token Variability: an Experimental and Modeling Study,” in *Proceedings of the 4th International Speech Motor Conference* (Nijmegen, Netherlands).

Niimi, S., Kumada, M., and Niitsu, M. (1994), “Functions of Tongue-Related Muscles during Production of the Five Japanese Vowels,” *Ann. Bull. RILP* **28**, 33–40, URL <http://www.umin.ac.jp/memorial/rilp-tokyo/>.

Nix, D. A., Papcun, G., Hogden, J., and Zlokarnik, I. (1996), “Two cross-linguistic factors underlying tongue shapes for vowels,” *J. Acoust. Soc. Am.* **99**, 3707–3717.

Otsuka, R., Ono, T., Ishiwata, Y., and Kuroda, T. (2000), “Respiratory-Related Genioglossus Electromyographic Activity in Response to Head Rotation and Changes in Body Position,” *Angle Orthod.* **70**, 63–69.

Payan, Y. and Perrier, P. (1997), “Synthesis of V-V sequences with a 2D biomechanical tongue model controlled by the equilibrium point hypothesis,” *Speech Commun.* **22**(2–3), 185–205.

Perkell, J. S. (1969), *Physiology of speech production: results and implication of a quantitative cineradiographic study*, MIT Press research monograph (Cambridge, Mass. M.I.T. Press).

Perkell, J. S. (1974), “A physiologically oriented model of tongue activity in speech production,” Ph.D. thesis, Massachusetts Institute of Technology, Boston, USA, URL <http://dspace.mit.edu/handle/1721.1/29190>.

Perkell, J. S. (1996), “Properties of the tongue help to define vowel categories: Hypotheses based on physiologically oriented modeling,” *J. Phonetics* **24**(1), 3–22.

Perkell, J. S., Guenther, F. H., Lane, H., Matthies, M. L., Perrier, P., Vick, J., Wilhelms-Tricarico, R., and Zandipour, M. (2000), “A theory of speech motor control and supporting data from speak-

ers with normal hearing and with profound hearing loss,” *J. Phonetics* **28**, 233–272.

Perkell, J. S. and Nelson, W. L. (1985), “Variability in production of the vowels /i/ and /a/,” *J. Acoust. Soc. Am.* **77**(5), 1889–1895.

Perrier, P. (2006), “About speech motor control complexity,” in *Speech Production: Models, Phonetic Processes, and Techniques*, edited by J. Harrington and M. Tabain (Psychology Press, New-York, USA), pp. 13–26.

Perrier, P., Ma, L., and Payan, Y. (2005), “Modeling the production of VCV sequences via the inversion of a biomechanical model of the tongue,” in *Proceedings of the 9th European Conference on Speech Communication and Technology (Interspeech’2005)* (Lisbon, Portugal), pp. 1041–1044.

Perrier, P., Ostry, D. J., and Laboissière, R. (1996), “The Equilibrium Point Hypothesis and Its Application to Speech Motor Control,” *J. Speech Hear. Res.* **39**, 365–378.

Perrier, P., Payan, Y., Zandipour, M., and Perkell, J. S. (2003), “Influence of tongue biomechanics on speech movements during the production of velar stop consonants: A modeling study,” *J. Acoust. Soc. Am.* **114**(3), 1582–1599.

Perrier, P., Perkell, J., Payan, Y., Zandipour, M., Guenther, F., and Khalighi, A. (2000), “Degrees of freedom of tongue movements in speech may be constrained by biomechanics,” in *Proceedings of the 6th International Conference on Spoken Language Processing, ICSLP’2000* (Beijing, China).

Sanguineti, V., Laboissière, R., and Ostry, D. J. (1998), “A dynamic biomechanical model for neural control of speech production,” *J. Acoust. Soc. Am.* **103**(3), 1615–1627.

Schwartz, J. L. and Escudier, P. (1987), *The Psychophysics of Speech Perception* (Martinus Nijhoff Publishers, Dordrecht), chap. Does the human auditory system include large scale spectral integration?, *Nato Asi*, pp. 284–292.

Shiller, D. M., Ostry, D. J., and Gribble, P. L. (1999), “Effects of Gravitational Load on Jaw Movements in Speech,” *J. Neurosci.* **19**(20), 9073–9080.

Shiller, D. M., Ostry, D. J., Gribble, P. L., and Laboissière, R. (2001), “Compensation for the effects of head acceleration on jaw movement in speech,” *J. Neurosci.* **21**(16), 6447–6456.

Slaughter, K., Li, H., and Sokoloff, A. J. (2005), “Neuromuscular organization of the superior longitudinalis muscle in the human tongue. 1. Motor endplate morphology and muscle fiber archi-



- tecture,” *Cells Tissues Organs* **181**(1), 51–64.
- Stone, M., Epstein, M. A., and Iskarous, K. (2004), “Functional segments in tongue movement,” *Clin. Linguist. Phon.* **18**(6–8), 507–521.
- Stone, M. and Lundberg, A. (1996), “Three-dimensional tongue surface shapes of English consonants and vowels,” *J. Acoust. Soc. Am.* **99**(6), 3728–3737.
- Stone, M., Stock, G., Bunin, K., Kumar, K., Epstein, M., Kambhamettu, C., Li, M., Parthasarathy, V., and Prince, J. (2007), “Comparison of speech production in upright and supine position,” *J. Acoust. Soc. Am.* **122**(1), 532–541.
- Takemoto, H. (2001), “Morphological analysis of the human tongue musculature for three-dimensional modelling,” *J. Speech Lang. Hear. Res.* **44**, 95–107.
- Tiede, M. K., Masaki, S., and Vatikiotis-Bateson, E. (2000), “Contrasts in speech articulation observed in sitting and supine conditions,” in *Proceedings of the 5th International Seminar on Speech Production*, pp. 25–28.
- van Eijden, T. M. G. J., Korfage, J. A. M., and Brugman, P. (1997), “Architecture of the human jaw-closing and jaw-opening muscles,” *Anat. Rec.* **248**(3), 464–474.
- Weir, A. D., McCutcheon, M. J., and Flege, J. E. (1993), “A comparison of formant frequencies for vowels pronounced in the supine and upright positions,” in *Proceedings of the Twelfth Southern Biomedical Engineering Conference*, pp. 188–190.
- Wilhelms-Tricarico, R. (1995), “Physiological modeling of speech production: methods for modeling soft-tissue articulators,” *J. Acoust. Soc. Am.* **97**(5 Pt 1), 3085–3098.
- Wilhelms-Tricarico, R. (2000), “Development of a tongue and mouth floor model for normalization and biomechanical modelling,” in *Proceedings of the 5th speech production seminar and CREST Workshop on models of speech production* (Kloster Seeon, Bavaria), pp. 141–148.
- Yuen, I., Lee, A., and Gibbon, F. (2007), “Lingual contact in selected English vowels and its acoustic consequence,” in *Proceedings of the 16th International Congress of Phonetic Sciences* (Saarbrücken, Germany).

TABLE I. Cross-sectional areas and corresponding force generation capacities ( $\rho$ ).

|                         | GGa | GGm | GGp | Sty | HG  | Vert | Trans | IL | SL | GH   | MH  |
|-------------------------|-----|-----|-----|-----|-----|------|-------|----|----|------|-----|
| Area (mm <sup>2</sup> ) | 82  | 55  | 168 | 109 | 295 | 91   | 227   | 41 | 86 | 80   | 177 |
| $\rho$ (N)              | 18  | 12  | 37  | 24  | 65  | 20   | 50    | 9  | 19 | 17.5 | 39  |

TABLE II. Final force levels (in Newtons) observed for every tongue and mouth floor muscle during the production of the French cardinal vowels and /ə/. The levels of force indicated correspond to the algebraic sum of the forces computed for every macrofiber. Gray cells represent voluntarily activated muscles.

| vowel | GGa  | GGm  | GGp   | Sty  | HG   | Vert | Trans | IL   | SL   | GH   | MH    |
|-------|------|------|-------|------|------|------|-------|------|------|------|-------|
| /i/   | 0.51 | 0    | 25.82 | 6.90 | 0    | 0    | 1.61  | 0    | 0    | 3.37 | 13.89 |
| /ə/   | 0.11 | 0.13 | 0.95  | 0.04 | 0.04 | 0.00 | 0.25  | 0    | 0.10 | 0.10 | 1.62  |
| /u/   | 0    | 0    | 6.73  | 7.42 | 0    | 0    | 1.83  | 0.47 | 0    | 1.02 | 6.79  |
| /a/   | 3.34 | 0    | 1.91  | 0    | 8.21 | 2.31 | 0     | 0.16 | 0    | 0    | 0.78  |

TABLE III. Motor commands used for the production of French cardinal vowels and for /ə/. These values are given as a percentage of the muscle length at rest. Values below 1 therefore correspond to a voluntary activation.

| vowel | GGa  | GGm  | GGp  | Sty  | HG   | Vert | Trans | IL   | SL   | GH   | MH   |
|-------|------|------|------|------|------|------|-------|------|------|------|------|
| /i/   | 1.03 | 1.05 | 0.60 | 0.90 | 1.23 | 1.13 | 1.05  | 1.02 | 1.09 | 0.76 | 0.75 |
| /ə/   | 0.98 | 0.98 | 0.98 | 1.00 | 1.00 | 1.00 | 1.00  | 1.00 | 1.00 | 0.98 | 0.94 |
| /u/   | 1.20 | 1.20 | 0.91 | 0.84 | 1.25 | 1.35 | 0.95  | 0.98 | 1.20 | 0.95 | 0.80 |
| /a/   | 0.75 | 1.10 | 1.00 | 1.10 | 0.70 | 0.85 | 1.30  | 1.00 | 1.20 | 1.05 | 1.05 |

TABLE IV. Lip aperture  $l_a$  and protrusion  $l_p$  chosen for the determination of the vocal tract area function (based on Abry *et al.*, 1980) and the values of the first four formants for the simulation of French oral vowels (extreme cardinal vowels and /ə/). These values were computed with the WinSnoori software.

| vowel | $l_a$ (cm <sup>2</sup> ) | $l_p$ (cm) | F1 (Hz) | F2 (Hz) | F3 (Hz) | F4 (Hz) |
|-------|--------------------------|------------|---------|---------|---------|---------|
| /i/   | 3                        | 0.5        | 321     | 2095    | 2988    | 4028    |
| /ə/   | 1.5                      | 0.8        | 502     | 1235    | 2407    | 3612    |
| /u/   | 0.3                      | 1.5        | 298     | 723     | 2547    | 3450    |
| /a/   | 4.5                      | 0.8        | 667     | 1296    | 2875    | 3948    |

TABLE V. Values of the first four formants based on acoustic data obtained for the speaker PB. The values were averaged over 10 repetitions of every one of the extreme cardinal vowels in different contexts.

| vowel | F1 (Hz) | F2 (Hz) | F3 (Hz) | F4 (Hz) |
|-------|---------|---------|---------|---------|
| /i/   | 311     | 2308    | 3369    | 4126    |
| /u/   | 285     | 792     | 2783    | 4055    |
| /a/   | 661     | 1291    | 2657    | 3717    |

TABLE VI. First, second and third formants computed after a local modification of the motor commands for vowel /i/. The formants for vowel /i/ are given in Table IV. The motor commands of the vowel /i/ were modified for 9 muscles independently and multiplied by  $\pm 2\%$ ,  $\pm 5\%$ ,  $\pm 8\%$  or  $\pm 10\%$ . The formants obtained following these modifications are given. In the  $\lambda$ -model, an increase in the motor commands corresponds to a decrease in the muscle activation; therefore a multiplication by  $+10\%$  corresponds to the lowest level of activation for a given muscle, whereas a multiplication by  $-10\%$  corresponds to the highest level of activation.

|              |            | F1 (Hz) | F2 (Hz) | F3 (Hz) |      |            | F1 (Hz)   | F2 (Hz) | F3 (Hz) |      |      |
|--------------|------------|---------|---------|---------|------|------------|-----------|---------|---------|------|------|
| <b>MH</b>    | <b>GGp</b> | +10%    | 350     | 2084    | 2942 | <b>GGm</b> | -2%       | 321     | 2085    | 2979 |      |
|              |            | +8%     | 340     | 2073    | 2931 |            | -5%       | 322     | 2057    | 2960 |      |
|              |            | +5%     | 332     | 2080    | 2950 |            | -8%       | 321     | 2019    | 2938 |      |
|              |            | +2%     | 326     | 2090    | 2976 |            | -10%      | 322     | 2001    | 2924 |      |
|              |            | -2%     | 317     | 2105    | 2992 |            | <b>HG</b> | -2%     | 320     | 2094 | 2986 |
|              |            | -5%     | 309     | 2102    | 3014 |            |           | -5%     | 323     | 2087 | 2973 |
|              |            | -8%     | 305     | 2102    | 3024 |            |           | -8%     | 326     | 2079 | 2963 |
|              |            | -10%    | 302     | 2111    | 3026 |            |           | -10%    | 331     | 2076 | 2957 |
|              | <b>GGa</b> | +10%    | 273     | 2078    | 3035 | <b>Sty</b> |           | +10%    | 272     | 2009 | 3017 |
|              |            | +8%     | 273     | 2078    | 3035 |            |           | +8%     | 278     | 2018 | 3000 |
|              |            | +5%     | 283     | 2082    | 3012 |            | +5%       | 296     | 2050    | 2994 |      |
|              |            | +2%     | 307     | 2099    | 3008 |            | +2%       | 311     | 2076    | 2981 |      |
|              |            | -2%     | 333     | 2082    | 2967 |            | -2%       | 334     | 2135    | 3003 |      |
|              |            | -5%     | 351     | 2071    | 2928 |            | -5%       | 348     | 2167    | 2924 |      |
| -8%          |            | 368     | 2062    | 2903    | -8%  |            | 360       | 2214    | 2814    |      |      |
| -10%         |            | 375     | 2049    | 2895    | -10% |            | 364       | 2251    | 2766    |      |      |
| <b>Trans</b> | +10%       | 329     | 2101    | 2977    | +10% | 316        | 2118      | 3049    |         |      |      |
|              | +8%        | 325     | 2096    | 2976    | +8%  | 317        | 2117      | 3043    |         |      |      |
|              | +5%        | 322     | 2095    | 2986    | +5%  | 318        | 2112      | 3027    |         |      |      |

|           |      |     |      |      |           |      |     |      |      |
|-----------|------|-----|------|------|-----------|------|-----|------|------|
|           | +2%  | 321 | 2095 | 2982 |           | +2%  | 320 | 2108 | 3004 |
|           | -2%  | 319 | 2091 | 2983 |           | -2%  | 321 | 2083 | 2966 |
|           | -5%  | 318 | 2100 | 2986 |           | -5%  | 321 | 2069 | 2944 |
|           | -8%  | 317 | 2096 | 2985 |           | -8%  | 321 | 2056 | 2920 |
|           | -10% | 316 | 2096 | 2980 |           | -10% | 319 | 2048 | 2913 |
| <b>IL</b> | -2%  | 321 | 2097 | 2980 | <b>SL</b> | -2%  | 322 | 2094 | 2989 |
|           | -5%  | 322 | 2094 | 2969 |           | -5%  | 327 | 2104 | 2977 |
|           | -8%  | 322 | 2098 | 2964 |           | -8%  | 342 | 2103 | 2958 |
|           | -10% | 321 | 2103 | 2958 |           | -10% | 346 | 2106 | 2912 |
|           |      |     |      |      |           |      |     |      |      |

## List of Figures

- FIG. 1 (color online) Mesh representation (gray elements) of lingual and mouth floor muscles as subsets of tongue elements (global mesh) (anterior oblique view). (a-c) anterior, medium and posterior part of the genioglossus, (d) styloglossus, (e) hyoglossus, (f) verticalis, (g) transversalis, (h) inferior longitudinalis, (i) superior longitudinalis, (j) geniohyoid, (k) mylohyoid. The muscle fibers are represented in red. The yellow squares and the blue dots represent the muscle insertions on the mandible and the hyoid bone, respectively. . . . . 7
- FIG. 2 (color online) Oblique anterior view of the 3D tongue mesh in the whole oral cavity for a rest position (tongue mesh in magenta, mandible in cyan, hyoid bone in yellow, translucent soft palate, pharyngeal and laryngeal walls in gray, infra- and supra-hyoid muscles represented as magenta lines). . . . . 8
- FIG. 3 (color online) Stress/strain hyperelastic constitutive law (Yeoh 2<sup>nd</sup> order material) for lingual tissues. The dotted curve represents the original law obtained from fresh cadaver tissues ( $c_{10} = 192$  Pa and  $c_{20} = 90$  Pa), the dashed curve the law used in the current model for passive tissues ( $c_{10} = 1037$  Pa and  $c_{20} = 486$  Pa) and the solid line the law used for the maximal activation ( $c_{10} = 10.37$  kPa and  $c_{20} = 4.86$  kPa). . . . . 10
- FIG. 4 Ratio damping over critical damping vs. frequency for  $\alpha = 40$  s<sup>-1</sup> and  $\beta = 0.03$  s (Rayleigh damping model). For a modal frequency from 3 to 10 Hz, the damping ratio is below 1.26, i.e. close to the critical damping (ratio equal to 1). . . . . 15

|        |   |    |
|--------|---|----|
| FIG. 5 | (color online) Impact of the activation of individual lingual and mouth floor muscles on tongue shape (400 ms command duration, sufficient to reach mechanical equilibrium). The contours of the articulators (tongue and hyoid bone in red, mandible, hard and soft palate, pharyngeal and laryngeal walls in black) are given in the midsagittal plane (tongue tip on the left). For every simulation, the target motor command of the only activated muscle equals 75% of the muscle length at rest, except for the activation of the long muscles Sty, IL and SL (85% of the muscle length at rest). The dotted contours correspond to the tongue shape in its rest position. . . . . | 22 |
| FIG. 6 | (color online) Impact of the activation of individual lingual and mouth floor muscles on tongue shape (400 ms command duration, sufficient to reach mechanical equilibrium) [frontal view]. For every simulation, the target motor command of the only activated muscle equals 75% of the muscle length at rest, except for the activation of the long muscles Sty, IL and SL (85% of the muscle length at rest). The shape of the tongue at rest is given for indication on the bottom right. . . .  | 23 |
| FIG. 7 | (color online) Final tongue shape for the simulation of the French cardinal vowels (first row: anterior oblique view, second row: posterior oblique view). . . . .  | 24 |
| FIG. 8 | Superimposition of the shape of the tongue for the speaker PB (CT data) (dense mesh) and the shape of the tongue obtained by simulation (coarse mesh) for vowel /i/. . . . .  | 25 |
| FIG. 9 | EPG data for American English vowels /i/ and /u/. Reprinted from Stone, M. and Lundberg, A., J. Acoust. Soc. Am., “Three-dimensional tongue surface shapes of English consonants and vowels”, 99(6), 3728-3737, 1996. Copyright 1996, Acoustical Society of America. . . . .  | 26 |

FIG. 10 (color online) Illustration of the contacts between the tongue dorsum and tongue tip, and surrounding structures of the vocal tract for vowels /i/ (a) and /u/ (b) (superior view, apex at the top). The surrounding structures, represented by translucent gray meshes, include the hard palate, the upper dental arch, the velum and the pharyngeal walls close to the velum. The entire tongue mesh is represented, but only the tongue surface elements used for the detection of potential contacts between the tongue and the surfaces listed above are colored. Red elements represent tongue surfaces in contact with the surrounding structures, yellow elements represent tongue surfaces close to the surrounding structures, and blue elements represent tongue surfaces far from the surrounding structures. . . . . 28

FIG. 11 (color online) Displacement scatter plots (black circles) for vowel /i/ in the midsagittal plane. Only the surface of the tongue is represented. Panel (a) summarizes the results obtained for the 9 muscles whose motor commands were modified. The  $3\sigma$  ellipses of dispersion (red) are also represented, and their major axes are drawn in blue. Panels (b-d) represent the dispersion obtained when modifying the motor commands of the posterior genioglossus (b), the anterior genioglossus (c) and the styloglossus (d) only. . . . . 35

FIG. 12 (color online) Final tongue position in the midsagittal plane for 1 s simulation under the influence of gravity alone. The neutral position of the tongue and the hyoid bone (rest position for a subject in upright position) is represented by a black dotted line, the final shape for the tongue and hyoid bone for a subject in upright position by a red dashed line, and for a subject in supine position by a blue solid line. The black solid lines correspond to the contours of the mandible, hard and soft palate, and pharyngeal and laryngeal walls. . . . . 38



FIG. 13 (color online) Final tongue position in the midsagittal plane for 1 s simulation under the influence of the reflex activation alone. The neutral position of the tongue and the hyoid bone (rest position for a subject in upright position) is represented by a black dotted line, the final shape for the tongue and hyoid bone for a subject in upright position by a red dashed line, and for a subject in supine position by a blue solid line. The black solid lines correspond to the contours of the mandible, hard and soft palate, and pharyngeal and laryngeal walls. . . . . 39